

# REPORT DOCUMENTATION PAGE

Form Approved  
OMB NO. 0704-0188

Public Reporting burden for this collection of information is estimated to average 1 hour per response, including the time for reviewing instructions, searching existing data sources, gathering and maintaining the data needed, and completing and reviewing the collection of information. Send comment regarding this burden estimate or any other aspect of this collection of information, including suggestions for reducing this burden, to Washington Headquarters Services, Directorate for Information Operations and Reports, 1215 Jefferson Davis Highway, Suite 1204, Arlington, VA 22202-4302, and to the Office of Management and Budget, Paperwork Reduction Project (0704-0188.) Washington, DC 20503.

1. AGENCY USE ONLY (Leave Blank)	2. REPORT DATE April 27, 2001	3. REPORT TYPE AND DATES COVERED Final 05 Feb 98 - 04 Feb 01
----------------------------------	----------------------------------	---

4. TITLE AND SUBTITLE Solar Driven Photooxidation Chemistry on TiO <sub>2</sub> Surfaces for Environmental Cleanup	5. FUNDING NUMBERS DAAG55-98-1-0070-0079
---	---

6. AUTHOR(S) John T. Yates, Jr.
------------------------------------

7. PERFORMING ORGANIZATION NAME(S) AND ADDRESS(ES) University of Pittsburgh, Department of Chemistry Pittsburgh, PA 15260	8. PERFORMING ORGANIZATION REPORT NUMBER
---	--

9. SPONSORING / MONITORING AGENCY NAME(S) AND ADDRESS(ES) U. S. Army Research Office P.O. Box 12211 Research Triangle Park, NC 27709-2211	10. SPONSORING / MONITORING AGENCY REPORT NUMBER 37659-CH .17
--	---

11. SUPPLEMENTARY NOTES  
The views, opinions and/or findings contained in this report are those of the author(s) and should not be construed as an official Department of the Army position, policy or decision, unless so designated by other documentation.

12 a. DISTRIBUTION / AVAILABILITY STATEMENT Approved for public release; distribution unlimited.	12 b. DISTRIBUTION CODE
---	-------------------------

13. ABSTRACT (Maximum 200 words)

Two areas of research are described: (1) Studies of the surface and photochemical properties of TiO<sub>2</sub> surfaces; (2) study of the factors influencing the use of carbon nanotubes for adsorption. This work connects to the use of TiO<sub>2</sub> and carbon nanotubes for environmental remediation. TiO<sub>2</sub> is shown to be an active material for photochemical oxidation of organophosphorous compounds; carbon nanotubes are strong adsorbents for small molecules which can fit into the nanotube interior.

14. SUBJECT TERMS TiO <sub>2</sub> ; photooxidation; carbon nanotubes; adsorbents	15. NUMBER OF PAGES 32
--	---------------------------

16. PRICE CODE
----------------

17. SECURITY CLASSIFICATION OR REPORT UNCLASSIFIED	18. SECURITY CLASSIFICATION ON THIS PAGE UNCLASSIFIED	19. SECURITY CLASSIFICATION OF ABSTRACT UNCLASSIFIED	20. LIMITATION OF ABSTRACT UL
---	--	---	----------------------------------

20010517 050

MASTER COPY: PLEASE KEEP THIS "MEMORANDUM OF TRANSMITTAL" BLANK FOR REPRODUCTION PURPOSES. WHEN REPORTS ARE GENERATED UNDER THE ARO SPONSORSHIP, FORWARD A COMPLETED COPY OF THIS FORM WITH EACH REPORT SHIPMENT TO THE ARO. THIS WILL ASSURE PROPER IDENTIFICATION. NOT TO BE USED FOR INTERIM PROGRESS REPORTS; SEE PAGE 2 FOR INTERIM PROGRESS REPORT INSTRUCTIONS.

MEMORANDUM OF TRANSMITTAL

U.S. Army Research Office  
ATTN: AMSRL-RO-BI (TR)  
P.O. Box 12211  
Research Triangle Park, NC 27709-2211

- |  |   |
|--|---|
| <input type="checkbox"/> Reprint (Orig + 2 copies) | <input type="checkbox"/> Technical Report (Orig + 2 copies)                 |
| <input type="checkbox"/> Manuscript (1 copy)       | <input checked="" type="checkbox"/> Final Progress Report (Orig + 2 copies) |
|  | <input type="checkbox"/> Related Materials, Abstracts, Theses (1 copy)      |

CONTRACT/GRANT NUMBER: DAAG55-98-1-0070 37659-CH

REPORT TITLE: Solar Driven Photooxidation Chemistry on  $TiO_2$  Surfaces for Environmental Cleanup

is forwarded for your information.

SUBMITTED FOR PUBLICATION TO (applicable only if report is manuscript):

Sincerely,

## Table of Contents

	<u>Page</u>
Accomplishments – September 1997 – March 2001	1
A. Introduction – An Overview of our Accomplished Research	1
B. NO Adsorption on TiO <sub>2</sub> [1]	2
C. NO Photochemistry on TiO <sub>2</sub> [2]	5
D. Photochemistry and Hydrolysis Chemistry of DMMP on TiO <sub>2</sub> [4,5]	10
1. Adsorption and Hydrolysis of DMMP on TiO <sub>2</sub> [4]	11
2. Photooxidation of DMMP on TiO <sub>2</sub> [5]	14
E. Adsorption and Photooxidation of CH <sub>3</sub> CN on TiO <sub>2</sub> [6]	16
F. Adsorption and Defect Site Measurements on Carbon Single Walled Nanotubes (SWNTs)[7-10]	19
G. Summary of Publication Activity: 1997-2001	30
H. Summary of External Interactions Involving U.S. Army Research Interests	32
1. Aberdeen Proving Ground	32
2. Guild Associates	32
I. Scientific Personnel Supported	32
J. Scientific Progress and Accomplishments	32

## Accomplishments- September 1997 – March 2001

### A. Introduction- An Overview of our Accomplished Research

A total of 14 papers have been published or submitted in the 34 month duration of this contract. The papers are related to two distinct areas of interest to ARO: (1) The mechanism of the photo-decomposition and photooxidation of environmentally important molecules on  $\text{TiO}_2$  surfaces; and (2) The study of surface phenomena related to nanotechnology, with a special focus on the properties of single walled carbon nanotubes (SWNTs).

In the work with  $\text{TiO}_2$  as a substrate for photochemistry, we have investigated the properties of both single crystal  $\text{TiO}_2$  as well as of powdered high area  $\text{TiO}_2$ . The measurements on the single crystal  $\text{TiO}_2$  permitted the determination of accurate cross sections for model photochemical processes. The measurements on  $\text{TiO}_2$  powder, using infrared spectroscopy, were able to disclose aspects of the mechanistic pathway for the photochemical reactions by means of the spectroscopic detection of surface intermediate species as well as gas phase species. The skills developed from the study of simple adsorbed molecules such as NO have been extended to the study of dimethyl methyl phosphonate (DMMP), where its destruction either by hydrolysis or by photooxidation has been witnessed on  $\text{TiO}_2$  powder surfaces. The DMMP molecule is a simulant for nerve agents, and our results show that photooxidation and hydrolysis are both routes to the destruction of this class of compounds on  $\text{TiO}_2$  surfaces.

In our work on SWNTs, we have studied the adsorption of Xe in the interior of the nanotubes and have measured the activation energy for Xe desorption. Recently, in separate measurements and also in simulations, our measurement of the Xe binding energy has been verified, and our conclusion that the Xe is adsorbed in the interior of the nanotubes at the measured density has also been verified. We found that the chemically cut nanotubes, prepared by Professor Smalley's research group, are highly defective. The defects consist of oxygenated carbon atoms, with C-O stretching frequencies characteristic of both -COOH and -C-O-C-groups. Removal of these groups (mainly as CO and  $\text{CO}_2$ ) by heating above 1000 K, leads to opening of the entry ports for adsorption, giving enhanced adsorption capacity and more rapid adsorption kinetics. Surprisingly, on two separate nanotube samples, we found that about 5% of the carbon atoms comprising the nanotubes are oxidized; this finding indicates that the walls are covered by oxidized carbon atoms at approximately a 5 atom % level. Thus the walls probably contain carbon vacancy defect sites whose boundaries are terminated by carboxylate groups and by ether-type linkages. This finding indicates that the electronic properties of SWNTs prepared in this manner and containing these high densities of defects will likely be strongly altered from the ideal properties expected.

In addition to the two main thrusts of the work, we have also carried out work in two other areas related to photochemistry and nanotechnology: (1) Recently, it was reported that cuprous oxide powder was effective in the photosplitting of water molecules. We carefully investigated this phenomenon on a  $\text{Cu}_2\text{O}$  film produced on the surface of a

Cu(111) single crystal. Absolutely no production of either hydrogen or oxygen gas was detected, and very low limits for the maximum possible cross section for water photosplitting were established; (2) We have used the STM to produce a nanostructure from the decomposition of an adsorbed organometallic molecule under the tip. Two different mechanisms for this process were discovered and characterized. In the first mechanism, electron attachment to the precursor molecule was shown to make pancake nanostructures about 40 nm in width. In the second mechanism, an electric field under the tip ( $>0.2 \text{ V/\AA}$ ) was found to produce sharp nanostructures about 8 nm in width. This understanding could be useful in the generation of quantum dots for research purposes.

### B. NO Adsorption on $\text{TiO}_2[1]$

NO is an important molecule from the point of view of its environmental impact as a component of NOX from vehicle emissions. It is also a simple molecule capable of detailed investigation theoretically and experimentally. First principles calculations based on density functional theory have been performed to determine the binding configuration and the binding energy for NO on the  $\text{TiO}_2(110)$  single crystal surface. As shown in Figure 1, the most stable configuration is a tilted one, with the NO molecules bound to surface Ti sites as Ti-NO species.

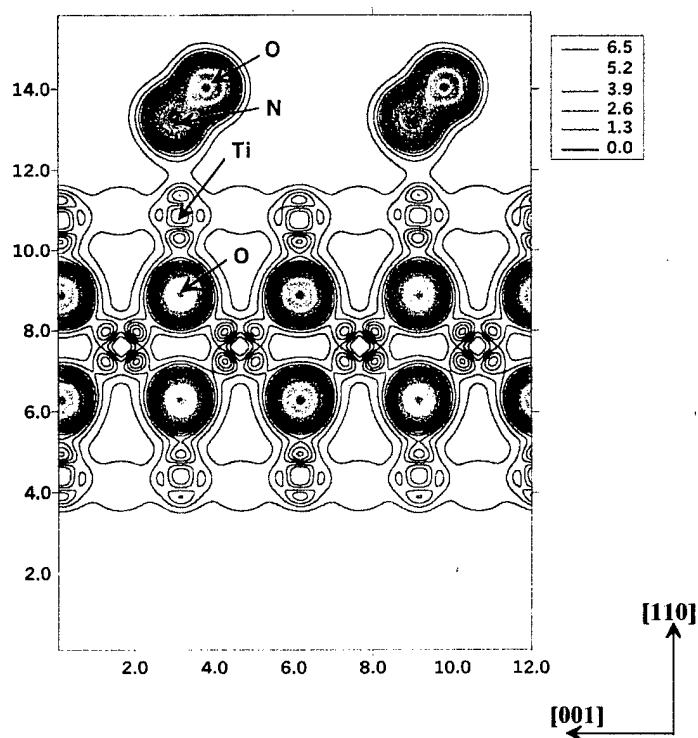


*Figure 1. Contour plots of the valence electron density for NO chemisorbed on  $\text{TiO}_2(110)$*

The calculated binding energy of the NO molecule is 43.7 kJ/mol at one-half the saturation coverage. Our experimental number, determined from temperature programmed desorption fits to a first-order kinetic model, yield an activation energy for desorption of 35.2 kJ/mole in the limit of zero coverage. The theoretical calculations indicate that at full coverage, an  $N_2O_2$  dimer will form, with the cis-ONNO configuration being favored. The contour plot of the valence electron densities for the dimer species is shown in Figure 2.

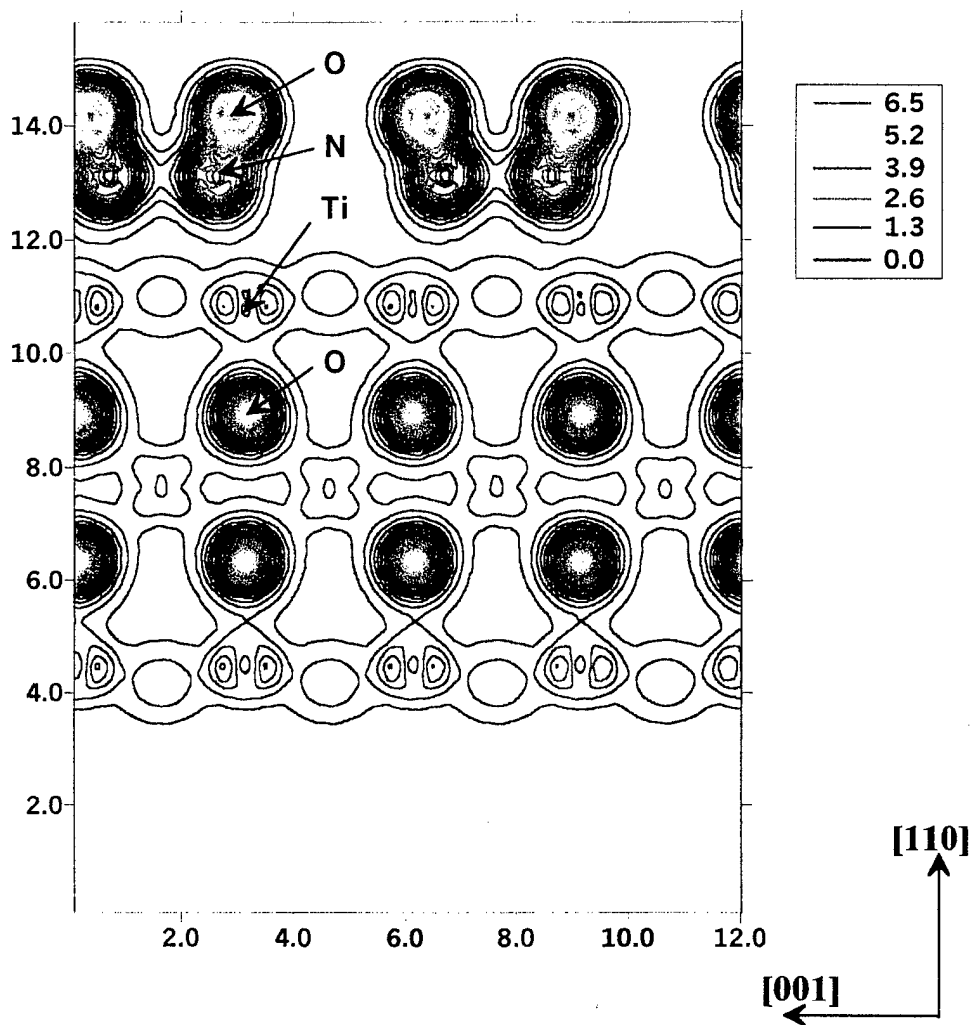


**Figure 2.** Contour plots of the valence electron density for  $N_2O_2$  chemisorbed on  $TiO_2(110)$ .

The temperature programmed desorption of NO from  $TiO_2(110)$  has been investigated as shown in Figure 3. Here the kinetic fit for first order desorption is shown in the insert to the figure.

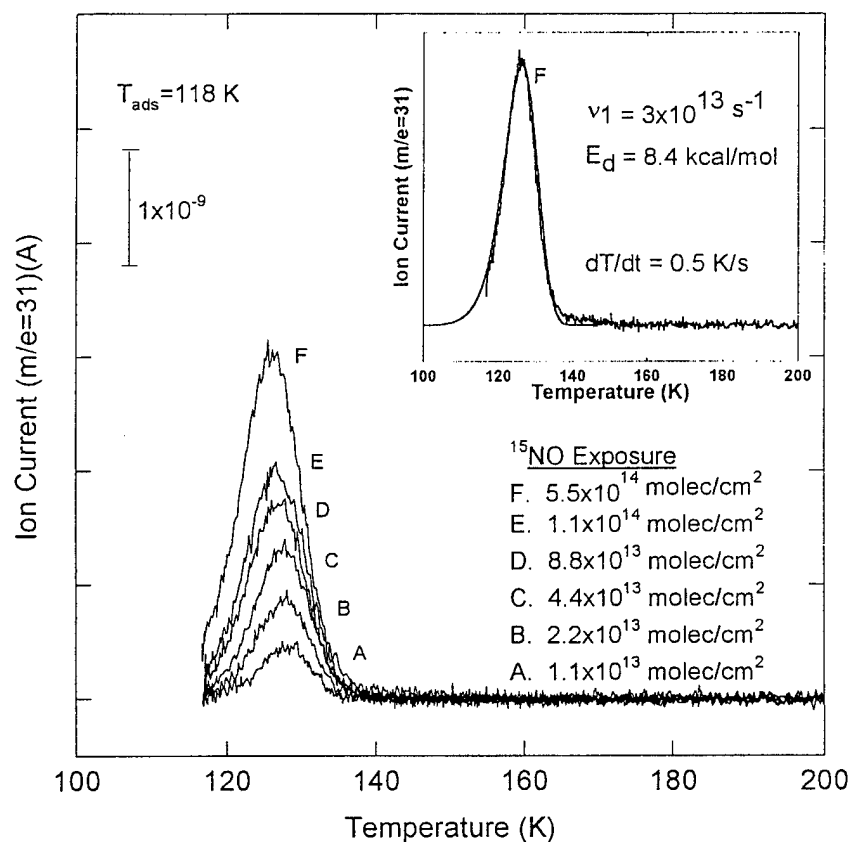


**Figure 3.** Temperature programmed desorption spectra for  $^{15}\text{NO}$  chemisorbed on  $\text{TiO}_2(110)$ .

While most of the NO desorbs without reaction, above a critical NO coverage a small part of the NO produces  $\text{N}_2\text{O}$  upon desorption. Figure 4 shows a plot of the yield of both molecules versus NO exposure; as the  $\text{N}_2\text{O}$  begins to be produced at higher coverages, there is an associated decrease in the NO yield. It is likely that the onset of NO dimer formation, predicted in the density functional calculations at high coverages, is associated with the  $\text{N}_2\text{O}$  product.

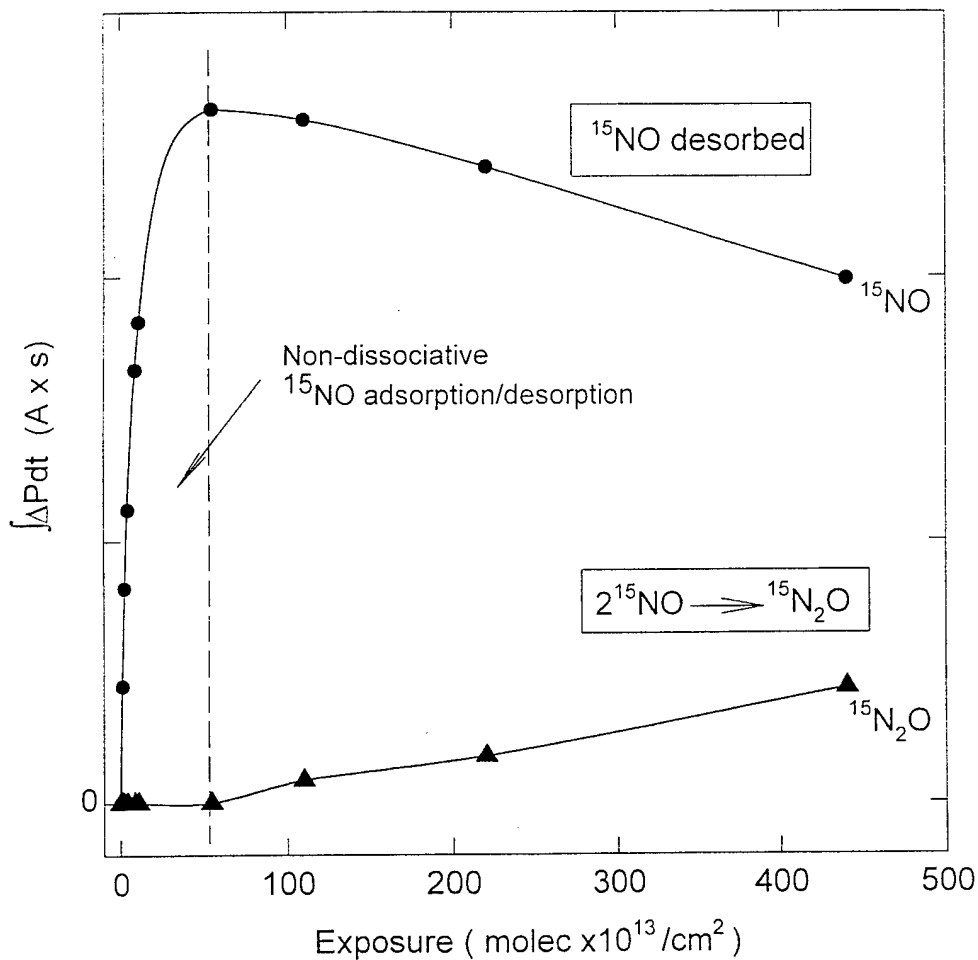
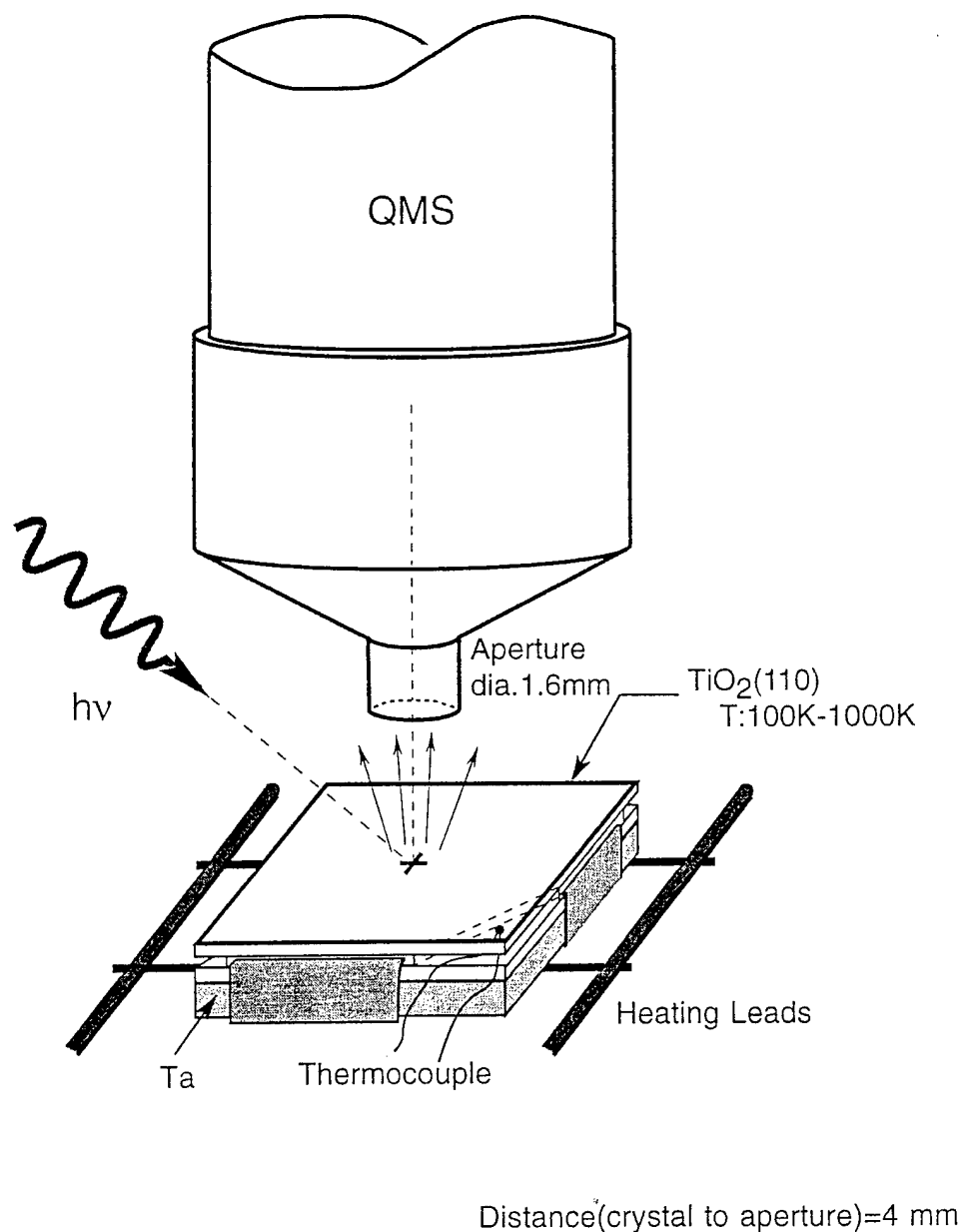


Figure 4.  $^{15}\text{NO}$  and  $^{15}\text{N}_2\text{O}$  thermal desorption yields as a function of  $^{15}\text{NO}$  exposure on  $\text{TiO}_2(110)$ .

### C. NO Photochemistry on $\text{TiO}_2$ [2]

The adsorption/thermal desorption studies outlined above form a good basis for the investigation of the photochemistry of NO on  $\text{TiO}_2$  surfaces. Figure 5 shows the apparatus used for the photochemistry measurements. Ultraviolet light,  $(3.96 \pm 0.07)$  eV, was incident on the crystal at a  $60^\circ$  angle and at a flux of  $6.3 \times 10^{14}$  photons/s  $\text{cm}^2$ . Desorbing gas was analyzed using a line-of-sight mass spectrometer enclosed in a pumped shield, and containing a small aperture on axis.



**Figure 5. Apparatus for photochemistry studies on  $\text{TiO}_2$  single crystals**

The rate of photodepletion of the adsorbate may be determined from the time constant of the exponential tail in the desorption pulse achieved by suddenly exposing the crystal to the UV light, as shown in Figure 6. Here it was found that the MAJOR photo-product was not NO, but instead it was  $\text{N}_2\text{O}$ . The initial time constant for the depletion of NO corresponded to the extremely high cross section of  $1 \times 10^{-15} \text{ cm}^2$  for the depletion

process, corresponding to a quantum efficiency near unity! In addition, a much less efficient process yields a small quantity of desorbing NO which desorbs in the later stages of N<sub>2</sub>O production. Kinetic analysis indicated that most of the photoproduced N<sub>2</sub>O remained as an adsorbed species on the surface at 118K.

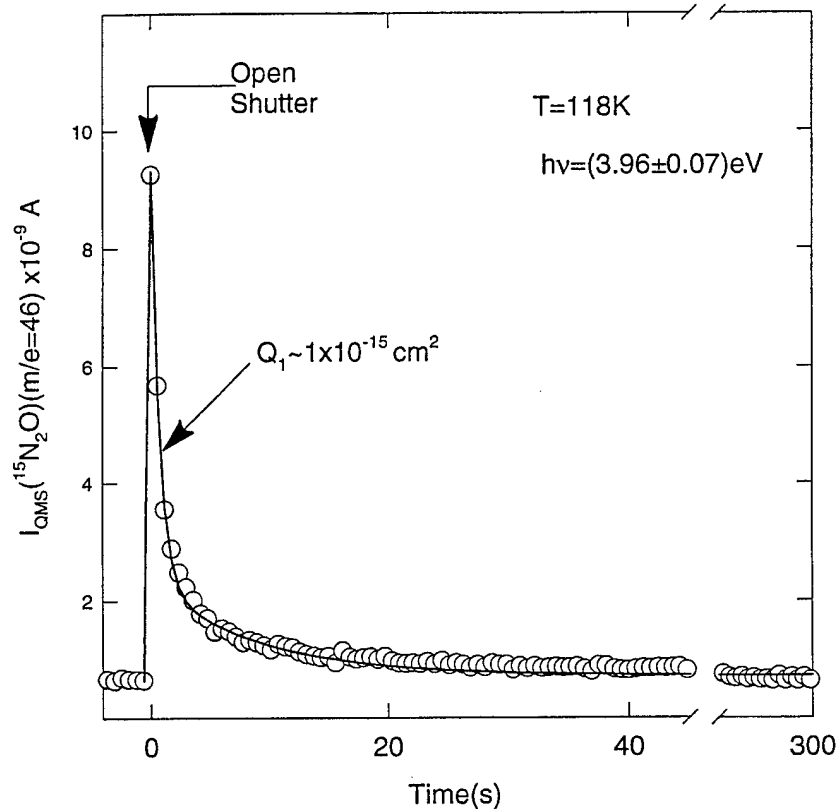
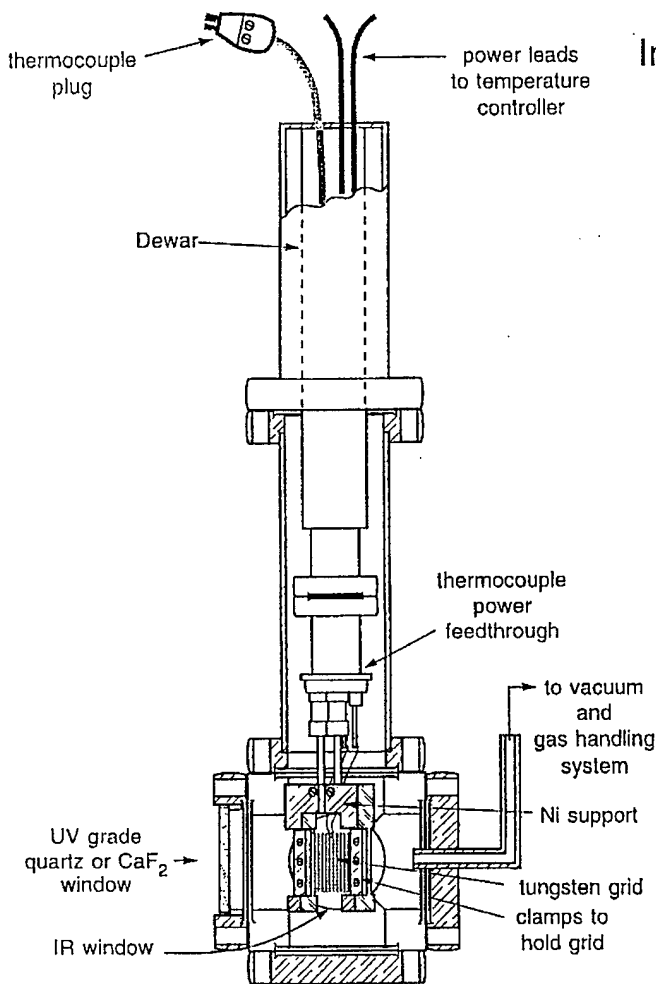


**Figure 6. NO Photochemistry on TiO<sub>2</sub>(110) – N<sub>2</sub>O Production.**

The photochemistry of NO on powdered TiO<sub>2</sub> was also investigated using transmission IR spectroscopy and the infrared cell shown in Figure 7. Here, by inclining the powdered sample, held on a tungsten grid, at a 45° angle to both the IR and the UV beams, it was possible to simultaneously witness the IR developments as the photochemistry takes place.



## Infrared Cell for Powdered Catalysts

### Optical Design for Simultaneous Photochemistry and IR Spectroscopy

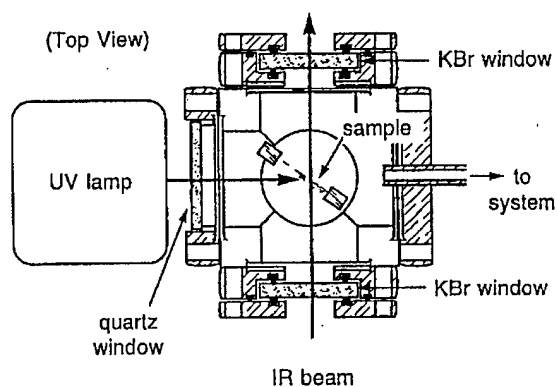


**Figure 7.** IR cell for simultaneous IR and UV photochemistry studies on  $\text{TiO}_2$  powder [3].

The IR studies on  $\text{TiO}_2$  powder confirmed the findings of the single crystal study previously shown. NO is consumed, and accompanying this process is the adsorption of much of the  $\text{N}_2\text{O}$  produced by NO photolysis at 110 K, confirming the conclusions reached in the single crystal studies. Figure 8 shows the simultaneous loss of NO mode intensity at  $1898\text{ cm}^{-1}$ ,  $1869\text{ cm}^{-1}$  and  $1734\text{ cm}^{-1}$ , accompanied by the production of  $\text{N}_2\text{O}$  modes at  $2258\text{ cm}^{-1}$ ,  $2237\text{ cm}^{-1}$ ,  $1255\text{ cm}^{-1}$  and  $1162\text{ cm}^{-1}$ .

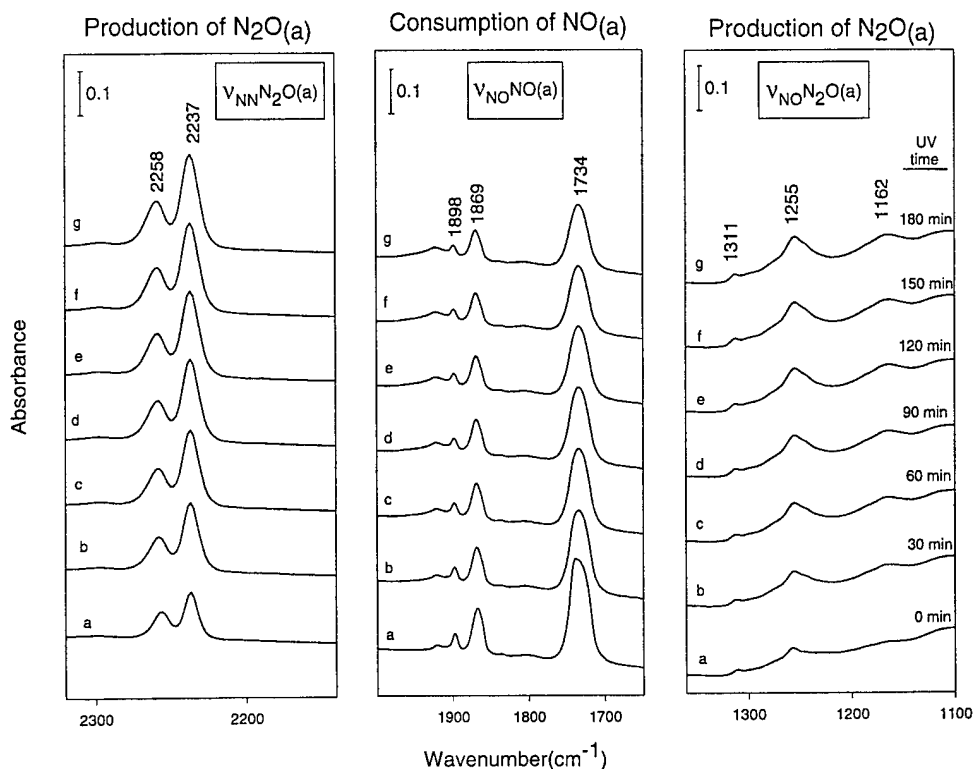


**Figure 8.** *NO photochemistry on TiO<sub>2</sub> powder, showing NO depletion and the concomitant production of adsorbed N<sub>2</sub>O at 110 K.*

A significant understanding of the penetration of the UV light into the powdered TiO<sub>2</sub> interior was achieved in these studies. The absorption of UV light by crystalline TiO<sub>2</sub> has an attenuation length of only about 200 Å. Yet the depletion of NO occurs to about 50% in these measurements, and this NO must come from a depth of the order of 200,000 Å which is about ½ of the powdered sample depth. This observation indicates that UV excitation extends deeply into the powdered sample, probably by light scattering in the powder. **THE OBSERVATION OF DEEP LIGHT PENETRATION MEANS THAT APPRECIABLE SURFACE AREA IS AVAILABLE FOR PHOTOCHEMISTRY IN POWDERED TiO<sub>2</sub> SAMPLES**, making powdered TiO<sub>2</sub> an efficient storage and photochemical substrate compared to expectations based on the absorbance of UV light only in the near surface region of TiO<sub>2</sub> crystals. To check that surface diffusion of NO from the interior of the powder to the near surface region is not responsible for this effect, a photodepletion experiment at 110 K was interrupted and an annealing procedure at 124 K was then carried out for 30 min to attempt to redistribute NO to the surface. If this had occurred, the rate of photolysis of the NO would have increased. Figure 9 shows that the rate of NO photolysis does not increase after annealing, nor does the rate of N<sub>2</sub>O production. Therefore diffusion of NO from the bulk into the outer regions of the TiO<sub>2</sub> powder is unlikely to be an explanation for our results.

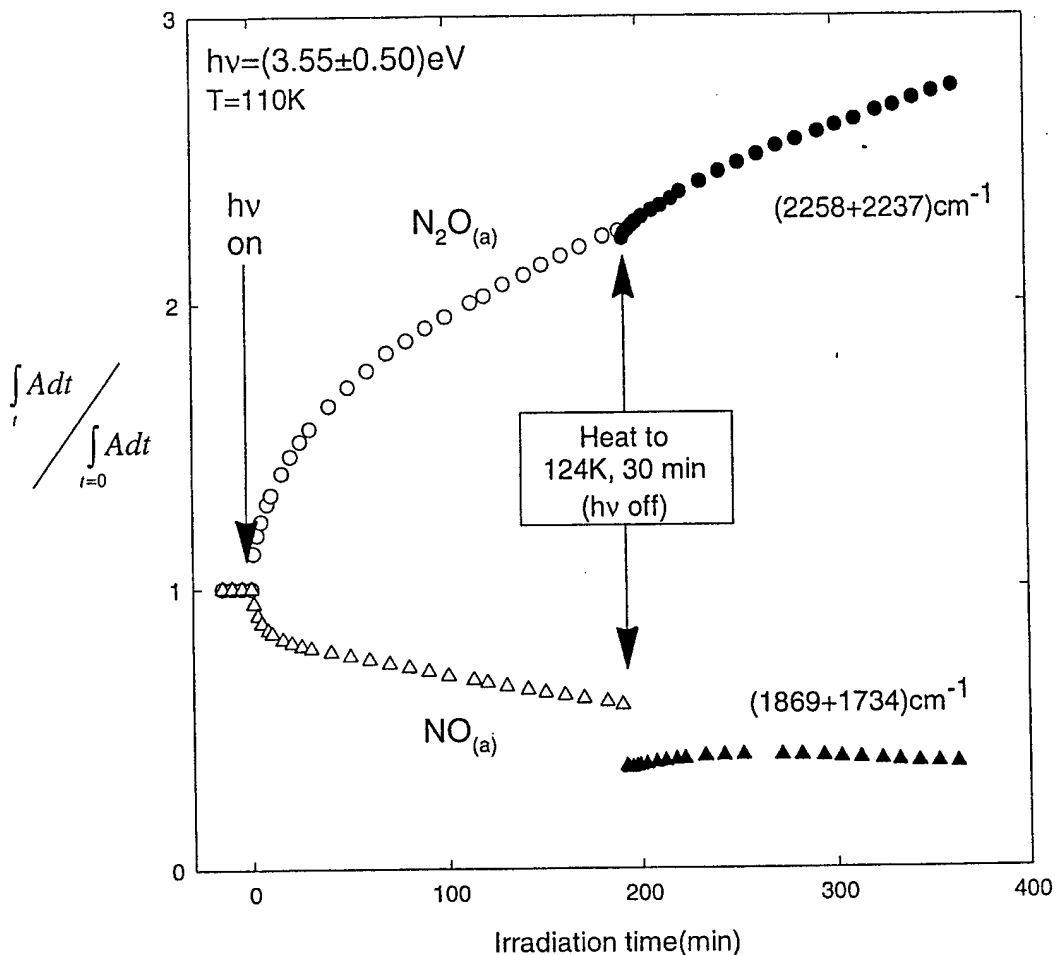


**Figure 9.** Photochemistry of NO on TiO<sub>2</sub> powder. A large decrease in the NO absorbance is accompanied by an increase in the absorbance of the N<sub>2</sub>O product. Annealing does not cause the rate of loss or the rate of growth of the absorbances to markedly change, suggesting that diffusional effects are not at work during photolysis. A model involving deep penetration of UV radiation by scattering through the particulate bed is proposed.

#### D. Photochemistry and Hydrolysis Chemistry of DMMP on TiO<sub>2</sub> [4,5]

The methods developed for the study of NO photodecomposition on powdered TiO<sub>2</sub> were applied to the photooxidation of DMMP. Prior to the photochemical studies, the hydrolysis of DMMP on the powdered TiO<sub>2</sub> surface was studied, so that conditions

could be used in the photochemical studies where thermally activated surface chemistry was not present. In other words, we studied the hydrolysis reaction and determined that it could be turned off at low temperatures, making studies of the pure DMMP photooxidation process possible.

### 1. Adsorption and Hydrolysis of DMMP on $\text{TiO}_2$ [4]

A novel method to spectroscopically observe the diffusion of the DMMP molecule through the pore structure of the  $\text{TiO}_2$  powder was devised. The isolated hydroxyl groups on the  $\text{TiO}_2$  surface bind to DMMP molecules, and exhibit a large frequency shift as a result of their hydrogen bonding. This conversion from isolated Ti-OH groups to groups associated with the DMMP molecule was investigated as a function of the temperature of the system, beginning with a condensed layer of DMMP ice which existed solely on the outer surface of the powder deposit. Figure 10 shows the gradual penetration of DMMP into the pore structure of the  $\text{TiO}_2$  powder, causing loss of intensity of the isolated Ti-OH groups above  $3600\text{ cm}^{-1}$ , and the production of the associated bands centered at about  $3400\text{ cm}^{-1}$  (left hand panel, Figure 10). In addition a softened P=O...HO mode is produced at  $1210\text{ cm}^{-1}$  as the  $1242\text{ cm}^{-1}$  mode due to P=O motion in DMMP ice disappears (right hand panel, Figure 10).

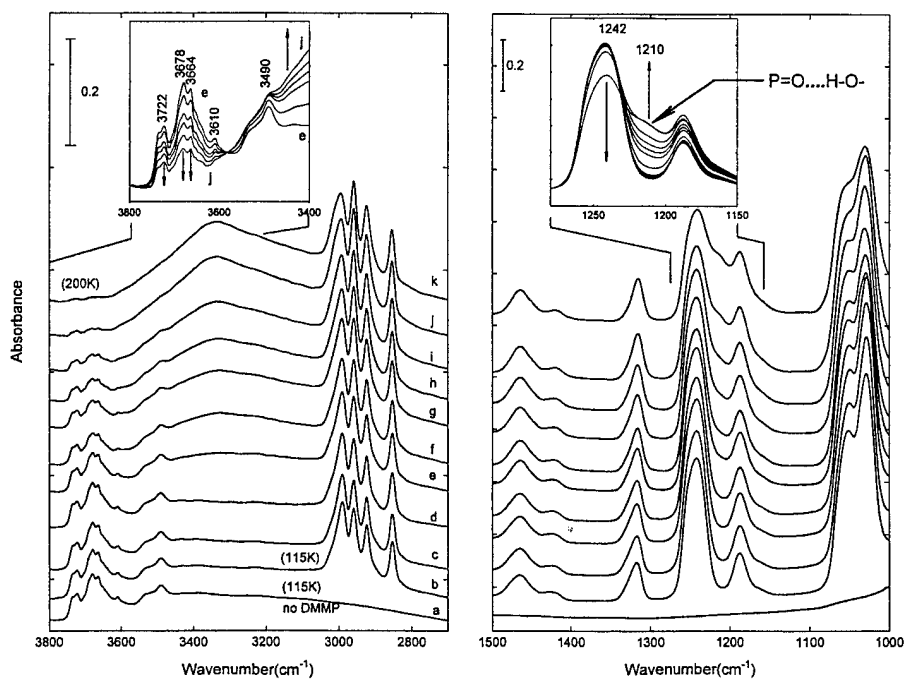


**Figure 10. Migration of DMMP into the pore structure of  $\text{TiO}_2$**

This DMMP association process with surface Ti-OH groups is complete at 200 K. Above 214 K, a second reaction occurs, in which the associated Ti-OH...DMMP species are depleted. The isolated Ti-OH species do not reappear, indicating that we are

observing the reaction of DMMP with the surface hydroxyls. This reaction produces adsorbed  $-OCH_3$  groups which have a characteristic methyl stretching mode at  $2827\text{ cm}^{-1}$  as seen in Figure 11. Other new vibrational modes are also observed as the DMMP molecule hydrolyzes via reaction of one or more of its methoxy groups.

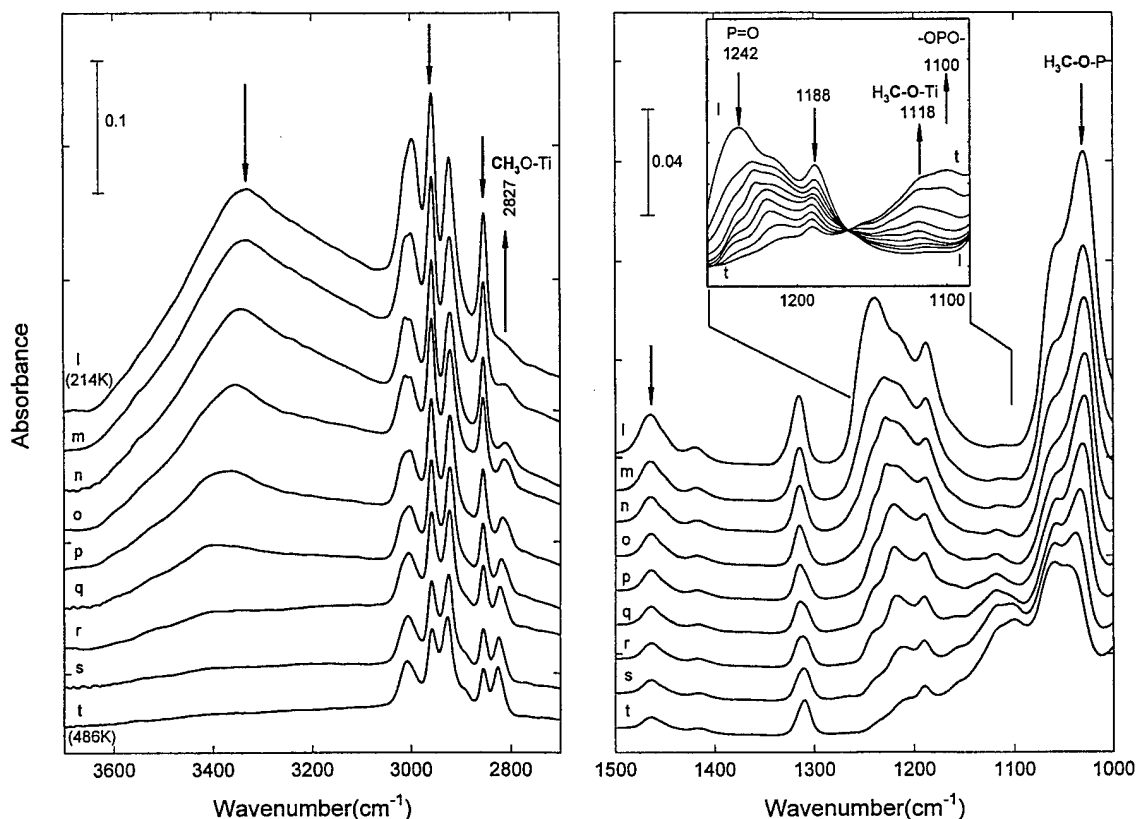


**Figure 11. Irreversible hydrolysis of DMMP on  $TiO_2$ , yielding surface methoxy groups.**

The initial adsorbed structures that are possible for DMMP are shown in Figure 12. We believe that structures (I) and (II) are most likely, based on the spectral shifts observed, and that structure (III) is unlikely because little interaction is observed spectroscopically leading to shifts in frequency of the  $-OCH_3$  modes.

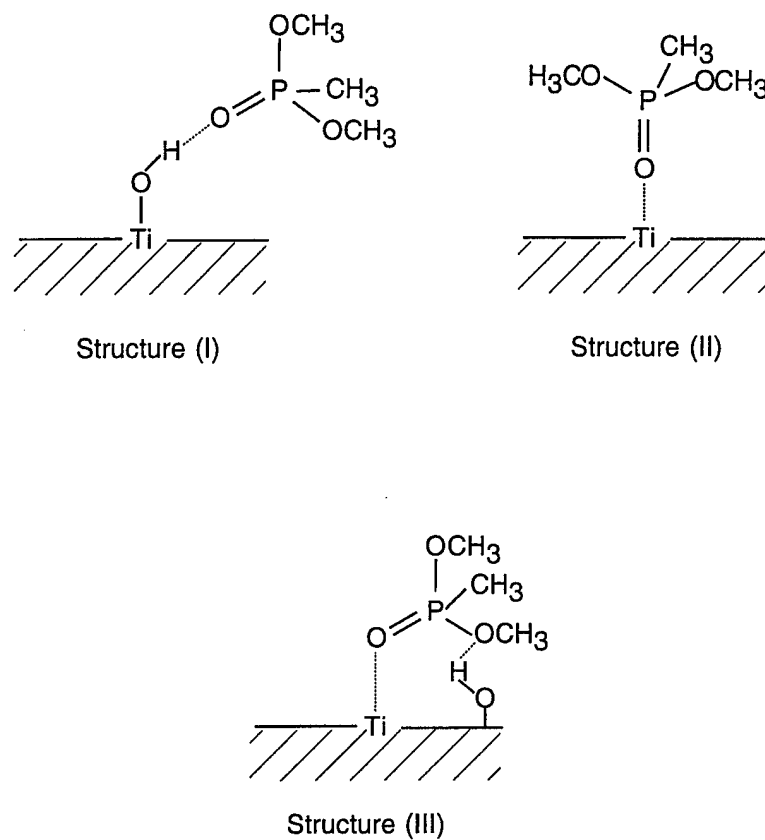
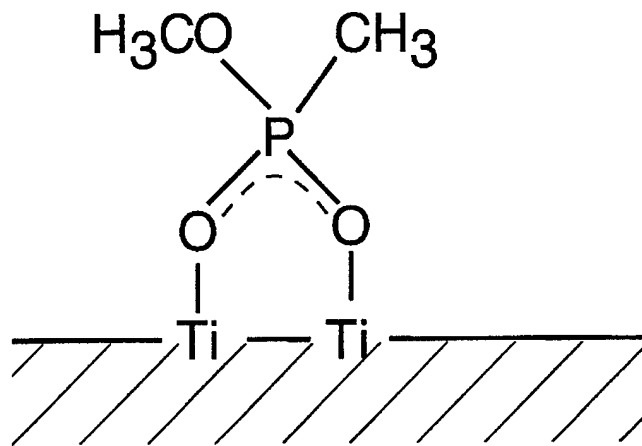


**Figure 12. Possible adsorption complexes for DMMP on  $TiO_2$**

Hydrolysis of the DMMP occurs via the methoxy groups, and the P-CH<sub>3</sub> moiety remains little influenced during this reaction. Therefore, the final product of hydrolysis at 486 K is likely to be the structure shown in Figure 13.



Structure IV(MMP)

Figure 13. Hydrolysis product of DMMP on TiO<sub>2</sub>

## 2. Photooxidation of DMMP on TiO<sub>2</sub> [5]

The work above has shown that hydrolysis of DMMP on TiO<sub>2</sub> occurs only above 214 K. Therefore, photooxidation studies were carried out at 200 K in order to investigate only the photochemistry, uncompromised by thermally-activated hydrolysis chemistry. Ultraviolet irradiation in the range  $h\nu = 2.1 - 5.0$  eV was carried out on a partial monolayer of DMMP adsorbed on powdered TiO<sub>2</sub>. Figure 14 shows the spectral developments which occur. Both the CH<sub>3</sub>-P and the CH<sub>3</sub>-O modes decrease together in absorbance as photooxidation occurs, indicating that the photooxidation process consumes both types of methyl-based functional groups on the DMMP molecule.

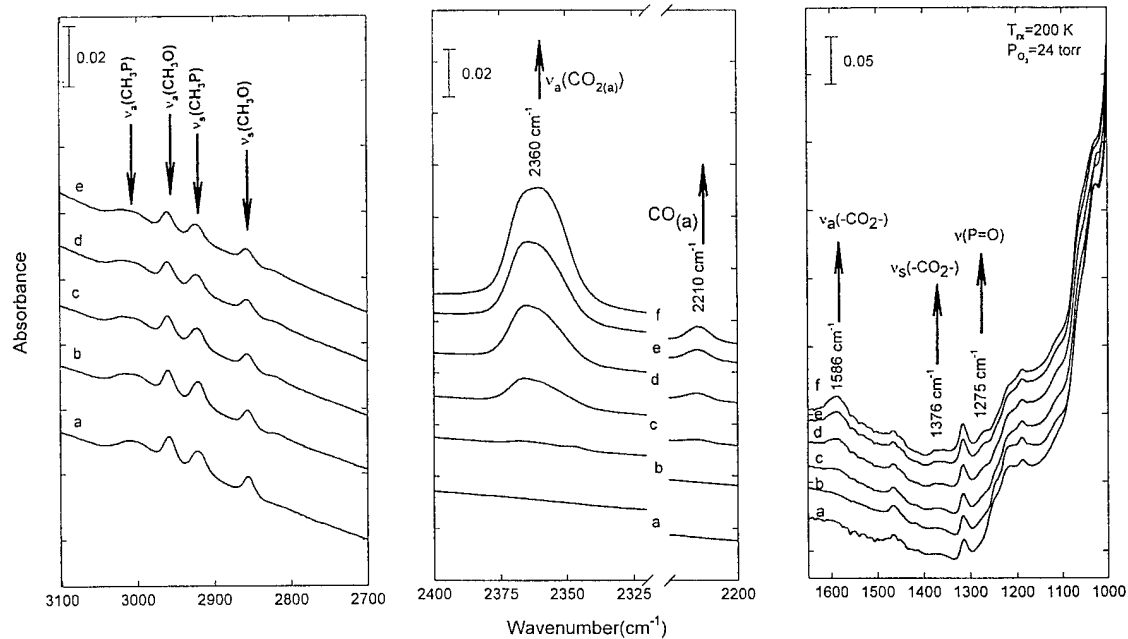


**Figure 14. DMMP Photooxidation on  $\text{TiO}_2$**

The products observed are adsorbed CO and  $\text{CO}_2$  as well as formate species, as shown in Figure 14. After long irradiation, evidence for the production of associated Ti-OH groups from the hydrogen moieties in DMMP has been seen. We also observe that a residual phosphate-type species remains on the surface following photooxidation. A schematic of the photooxidation reaction and the products is shown in Figure 15.

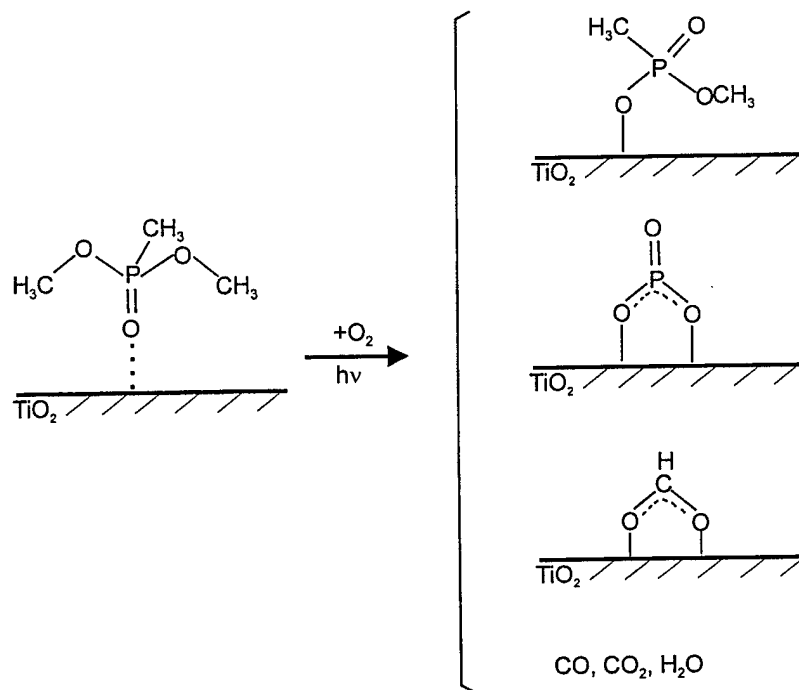


*Figure 15. Schematic of the Photooxidation Reaction of Adsorbed DMMP on  $\text{TiO}_2$ .*

### E. Adsorption and Photooxidation of $\text{CH}_3\text{CN}$ on $\text{TiO}_2$ [6]

The methyl cyanide molecule, while not a poisonous compound, presents the CN functional group which is of interest from an environmental point of view. This molecule offers the opportunity to compare the rate of the photooxidation chemistry of the methyl group with that of the cyanide group. One of the striking features of the photooxidation of  $\text{CH}_3\text{CN}$  is the production of surface Ti-NCO species as an intermediate in the process. Without showing the series of spectral developments, Figure 16 shows clearly the consumption of the  $\text{CH}_3\text{CN}$  molecule and the production of surface-bound Ti-NCO intermediate. The Ti-NCO is itself photooxidized upon long exposure to UV light and oxygen gas.

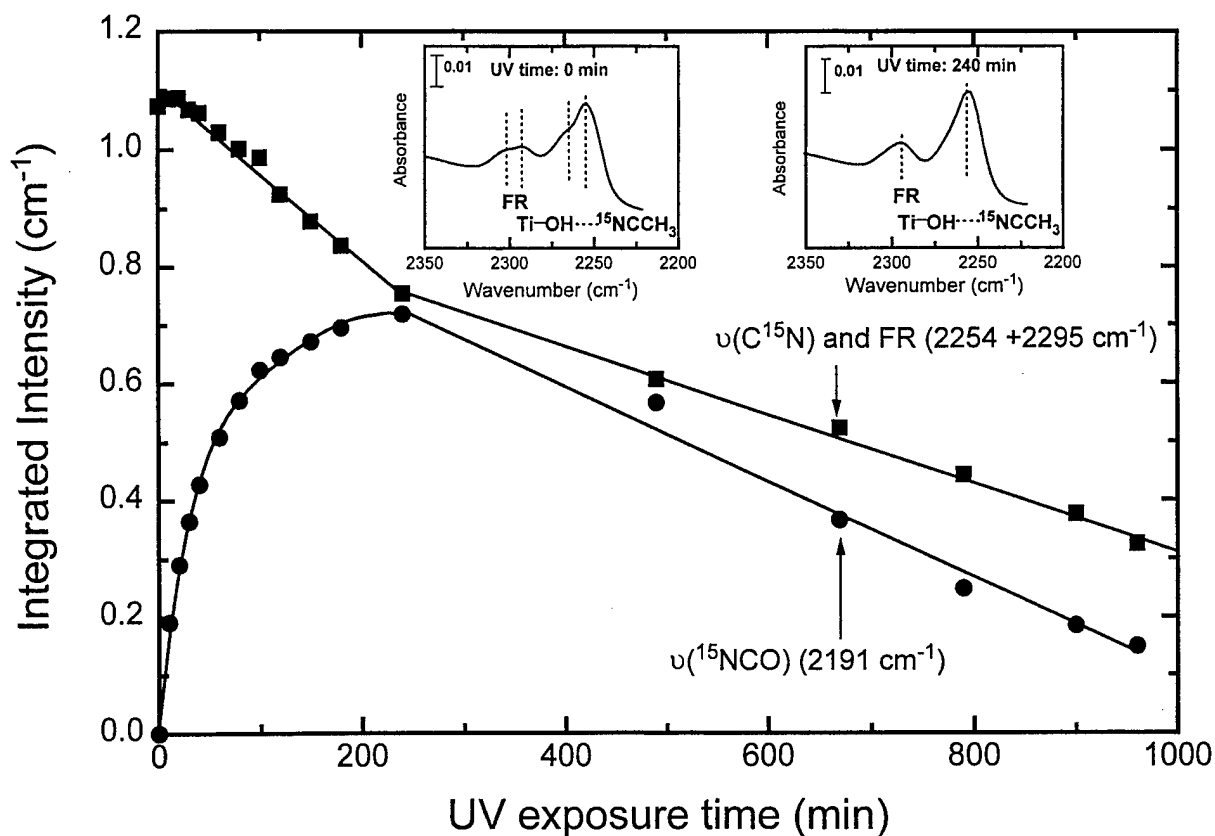
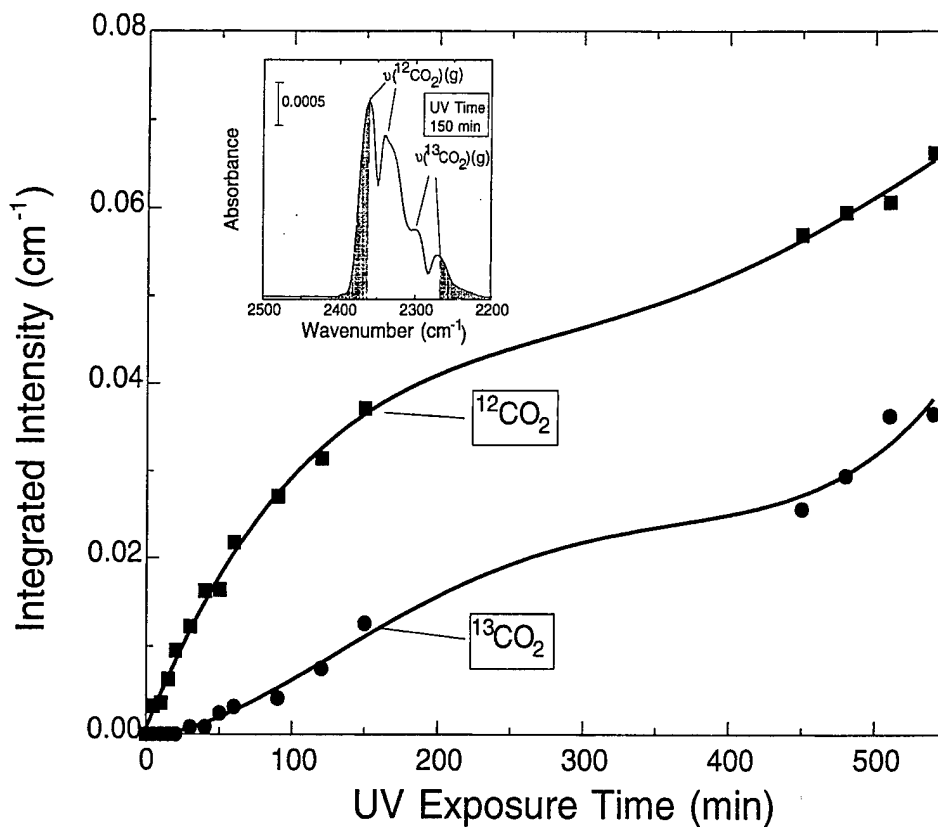


Figure 16. Kinetic plot of the absorbance due to parent  $\text{CH}_3\text{C}^{15}\text{N}$  and product  $^{15}\text{NCO}$  during photooxidation over  $\text{TiO}_2$ .

Since both of the functional groups in methyl cyanide,  $\text{CH}_3$  and  $\text{CN}$ , contain carbon atoms, we were able to determine which group was more reactive to produce the final oxidation product,  $\text{CO}_2$ . This was done by using  $\text{CH}_3^{13}\text{CN}$  and observing with infrared spectroscopy the isotopic composition of the evolved  $\text{CO}_2$  gas. Figure 17 shows a curious effect: The production of  $^{13}\text{CO}_2$ , originating from the  $^{13}\text{CN}$  group, is delayed compared to  $^{12}\text{CO}_2$  during the photooxidation reaction. This observation is consistent with the retention of the  $\text{Ti-NCO}$  species on the surface as an intermediate, retarding its conversion to  $\text{CO}_2$ , compared to the  $\text{CH}_3$  group which is more quickly oxidized photochemically.



**Figure 17.** Kinetic plot of the production of isotopic  $\text{CO}_2$  species from the photooxidation of  $\text{CH}_3^{13}\text{CN}$  on  $\text{TiO}_2$ .

Further isotopic studies involving  $^{18}\text{O}_2$  and  $\text{Ti}^{16}\text{O}_2$  have shown that the abstraction of a lattice  $^{16}\text{O}$  atom occurs as the photooxidation of  $\text{CH}_3\text{CN}$  proceeds. This effect is thought to occur as a Ti-CN species, produced as a result of the preferential oxidation of the  $\text{CH}_3$  group, attacks an oxygen site on the surface making a Ti-NCO species which is observed spectroscopically to be produced. A schematic reaction mechanism summarizing this work is given in Figure 18.

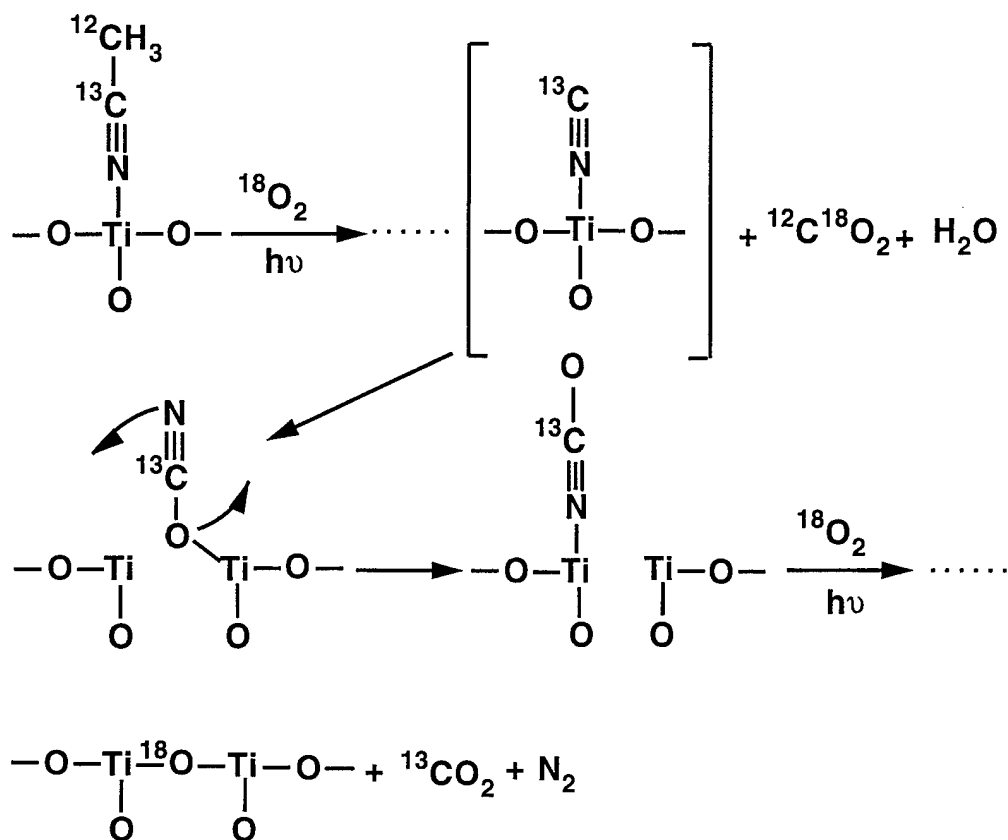


Figure 18. Schematic of the proposed mechanism of  $\text{CH}_3\text{CN}$  photooxidation on  $\text{TiO}_2$ .

In summary, the use of infrared spectroscopy to understand the details of the  $\text{TiO}_2$ -mediated photooxidation of both simple and complex adsorbed molecules has been successfully demonstrated. Surface-bound intermediate species, different elementary process rates, and reactions of active intermediates with the  $\text{TiO}_2$  lattice have been observed. In addition, by careful attention to thermal processes which may compete with photochemical processes, we have been able to experimentally separate the two by working at low temperatures where thermal processes are frozen out.

#### F. Adsorption and Defect Site Measurements on Carbon Single Walled Nanotubes (SWNTs) [7-10]

During the latter portion of this grant period, we refocused our work on studies of adsorption inside of single walled nanotubes. The work has been done in collaboration with Professor Richard Smalley and his students and postdoctorals at Rice University.

They have supplied carefully characterized samples of SWNTs. The procedure devised at Rice for cutting and opening the ends of the nanotubes involves treatment under oxidizing conditions ( $\text{HNO}_3/\text{H}_2\text{SO}_4$ ) to remove non-SWNT carbon, followed by  $\text{HNO}_3/\text{H}_2\text{O}_2$  treatment for cutting. Figure 19 shows the length distribution of the opened-SWNTs (o-SWNT) as measured at Rice.

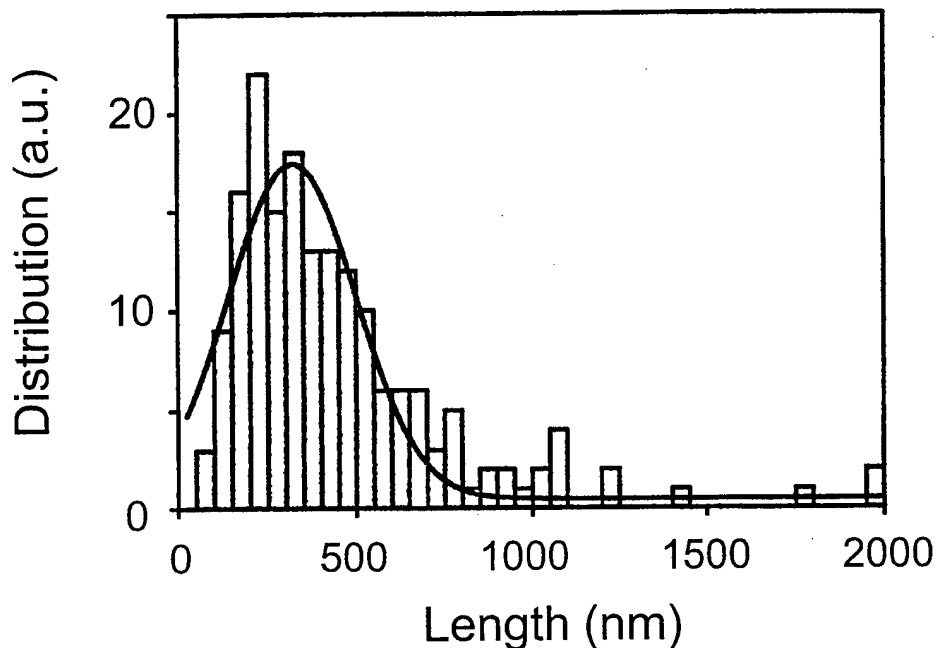


*Figure 19. Length distribution for o-SWNTs prepared by  $\text{HNO}_3/\text{H}_2\text{O}_2$  treatment [7].*

We devised a version of the temperature programmed desorption (TPD) technique to study the adsorption of Xe gas in the nanotubes at 95 K. A 10-50 microgram quantity of sample is supported on a Au-covered Ta support foil and may be exposed to a molecular beam of Xe using a calibrated and collimated doser. The sample, after exposure, is rotated to the mass spectrometer aperture, and TPD is performed. High quality control experiments, sampling a blank Au/Ta foil, similarly exposed to Xe, are also performed for each experiment to assure that the Xe desorption is being observed from the SWNT sample. The apparatus constructed for this work is shown in Figure 20.

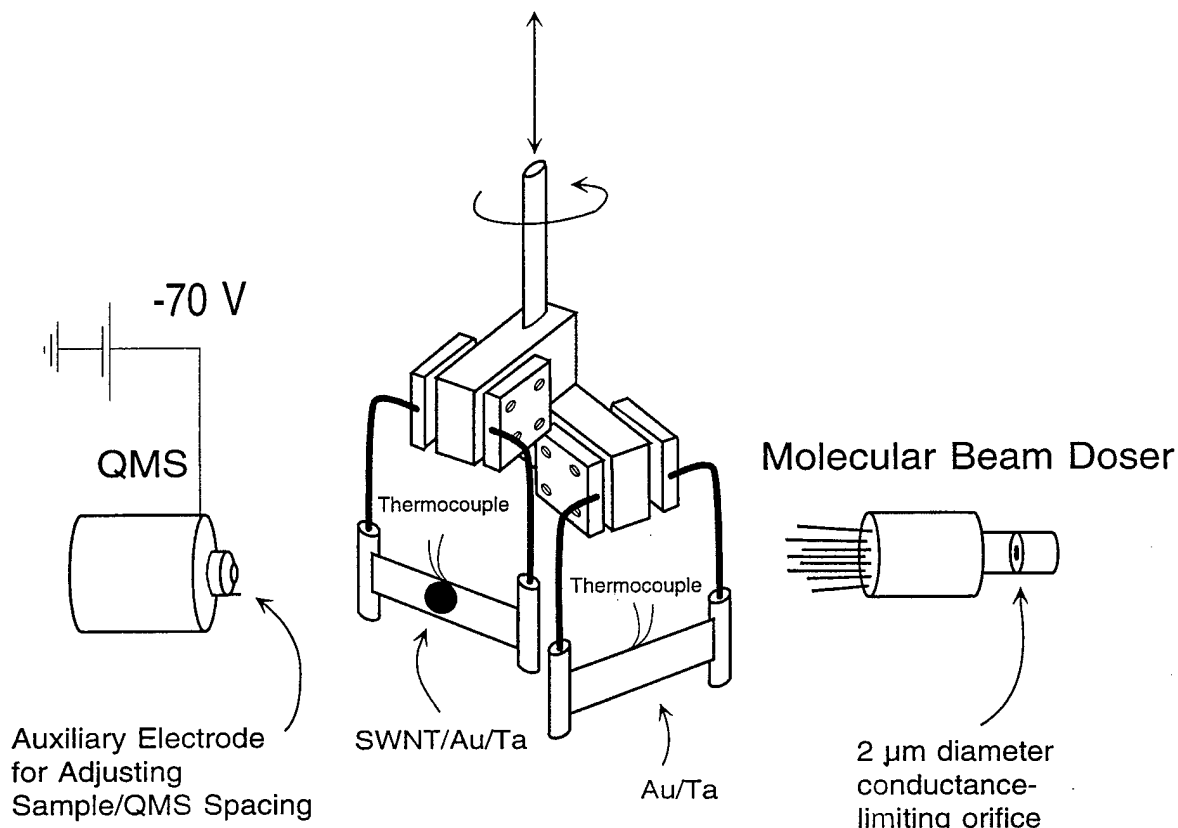


**Figure 20. Apparatus for using TPD to observe adsorption in SWNTs [7]**

It was found that the o-SWNTs prepared by the oxidizing procedures were capable of adsorbing only a small amount of Xe at the exposures employed in this work. However, upon annealing to 1073 K, where CO<sub>2</sub> and CO are observed to desorb, the capacity of the o-SWNTs for Xe adsorption increased by about 20 fold. The experimental Xe desorption data are shown in Figure 21 for an o-SWNT sample before and after activation at 1073 K.

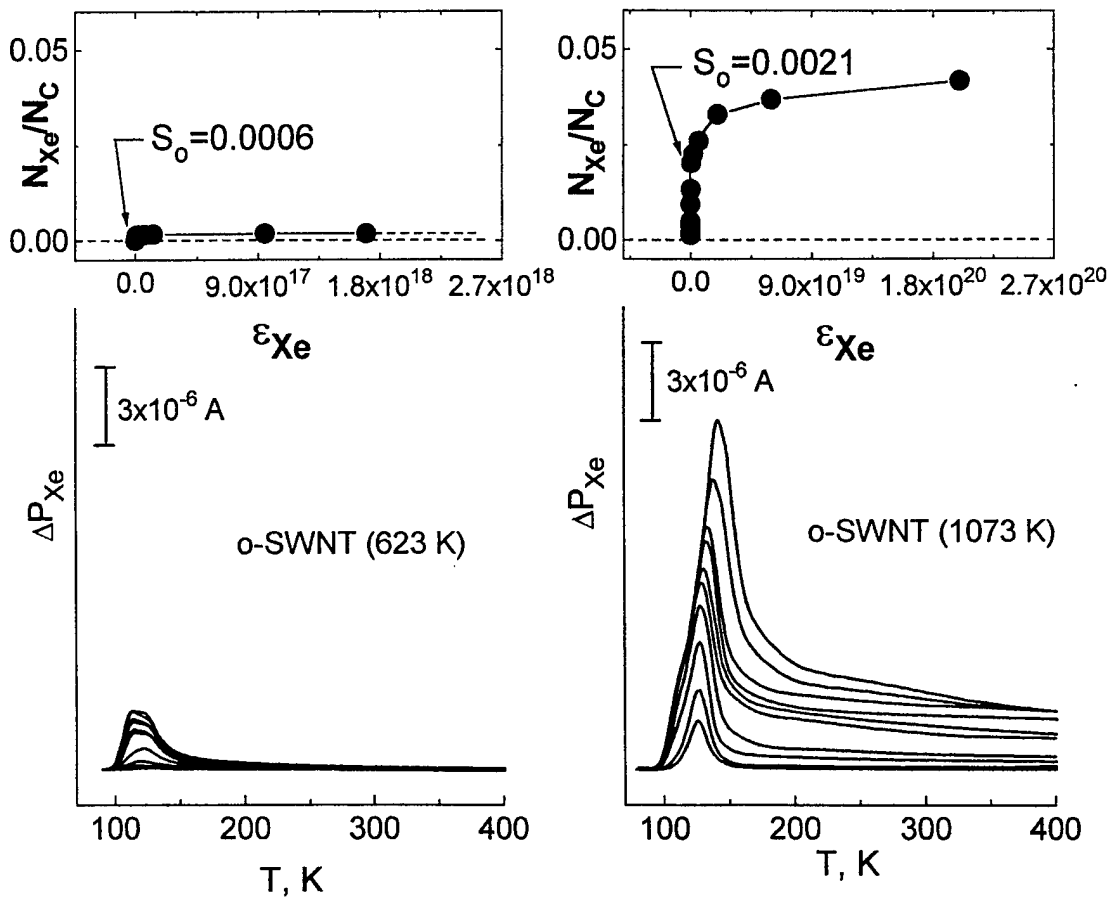
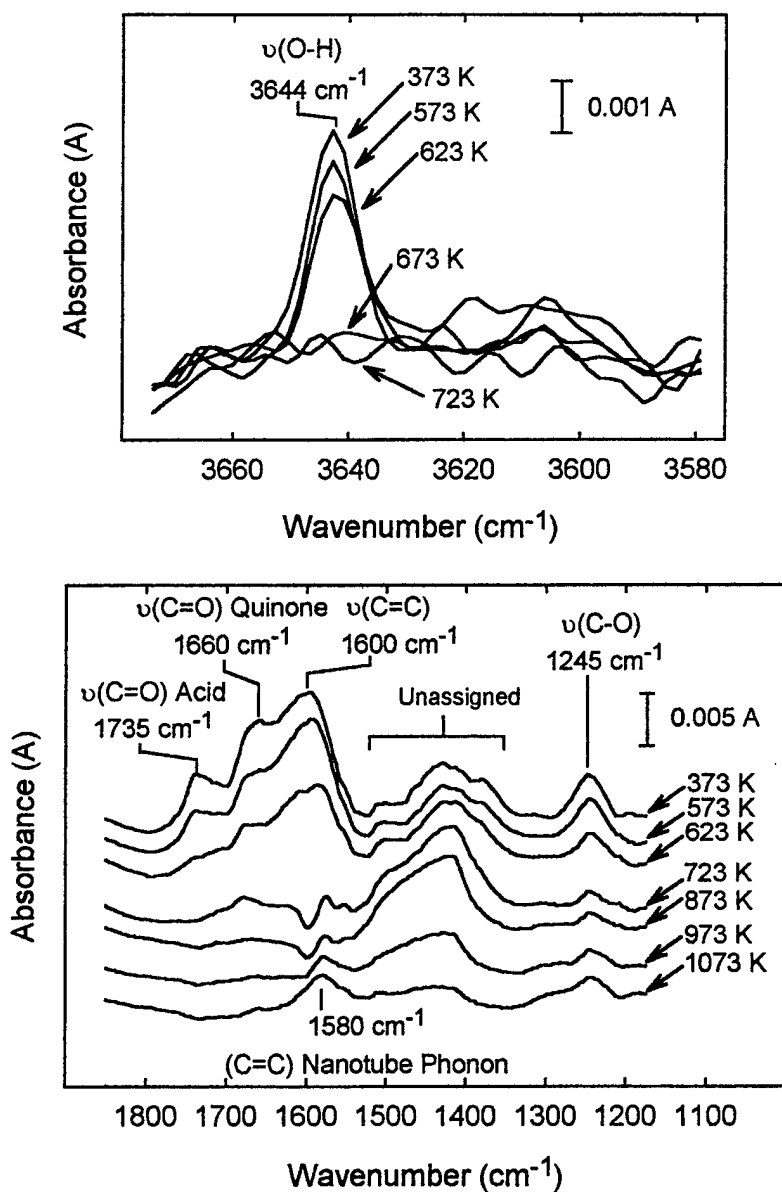


Figure 21. Temperature programmed desorption of Xe from o-SWNTs [7]

Transmission infrared spectroscopy measurements were also made on the SWNT samples, and C-O stretching modes assigned to quinone, ether, and carboxylate linkages were observed on the o-SWNTs prior to 1073 K treatment in vacuum. In addition, the -OH mode of the -COOH groups was detected. Most of these modes are removed upon annealing to 1073 K in vacuum, as shown in Figure 22.



**Figure 22. Decomposition of oxygen-containing functionalities upon heating o-SWNTs in vacuum [8]**

It is apparent from the information above that the -COOH and other groups are effective at blocking Xe adsorption. A schematic diagram of the blocking action of these groups at the ends of the 13.6 Å diameter 10,10 SWNTs is shown in Figure 23.

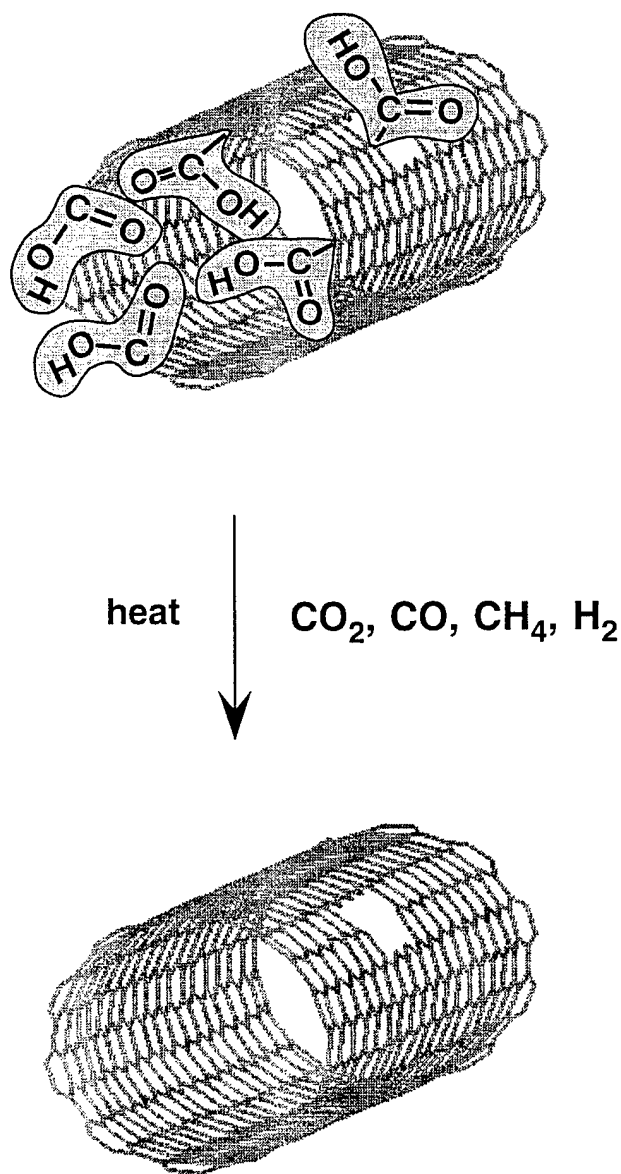


**Figure 23.** Schematic blocking of entry ports into the interior of o-SWNTs, and the removal of -COOH groups by heating in vacuum

The o-SWNT samples have been carefully characterized by several methods, including XPS which detects about 0.03 atomic percent O still remaining after 1073 K heating. The most informative measurement, using Raman spectroscopy, shows that the expected radial vibrational modes of the SWNTs are not influenced by heating to 1073 K, as shown in Figure 24. This means that the annealing has not destroyed the basic tubular graphene structure of the SWNTs.

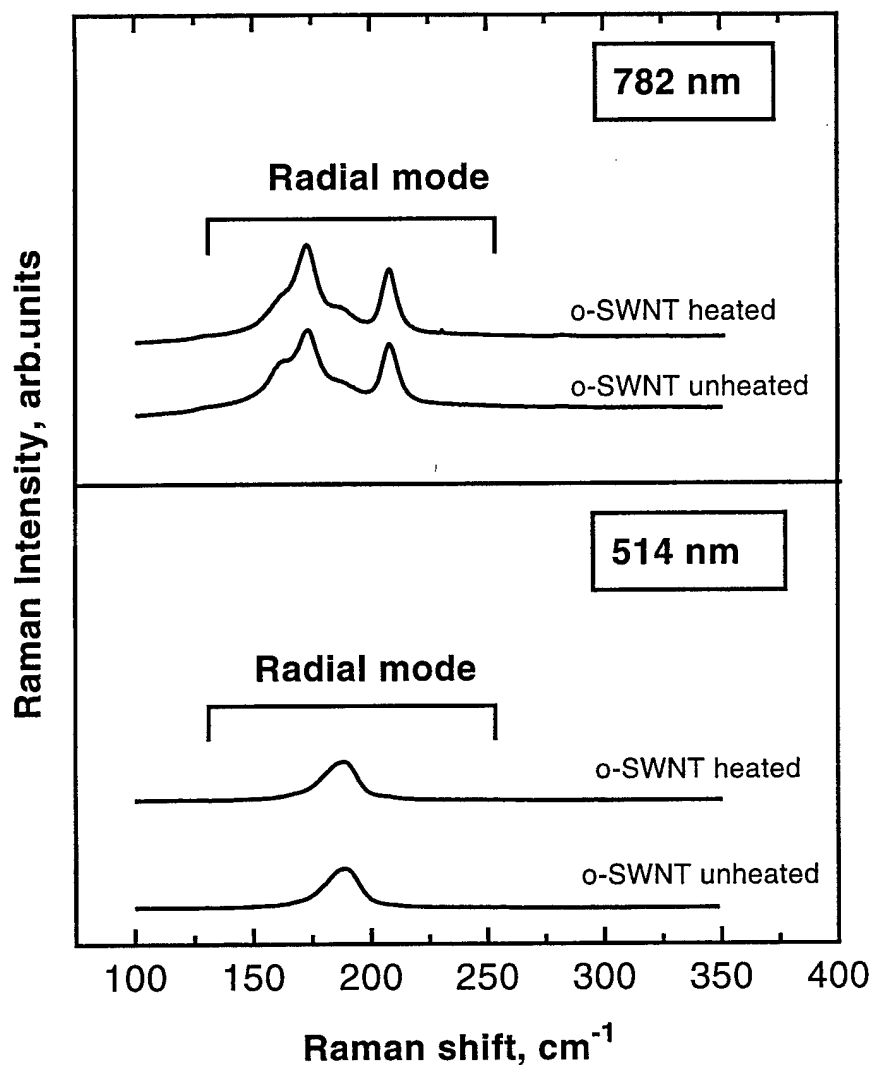


*Figure 24. Raman spectral comparison of o-SWNTs before and after heating in vacuum to 1073 K [7].*

We performed a leading-edge kinetic analysis of the Xe TPD spectra in order to derive the activation energy for desorption. From the results shown in Figure 25, it is seen that the energy versus coverage converges to a value of  $26.8 \pm 0.6$  kJ/mol. This value is higher than the enthalpy of sublimation of Xe(s) which is 14.2 kJ/mol, and reflects the extra binding energy afforded by interaction with the inner SWNT wall. Recent molecular simulations [9] of this interaction yields an adsorption heat of 23.5 kJ/mol, in the coverage range comparable to the experiments, in excellent agreement with the value we measured experimentally (26.8 kJ/mol).

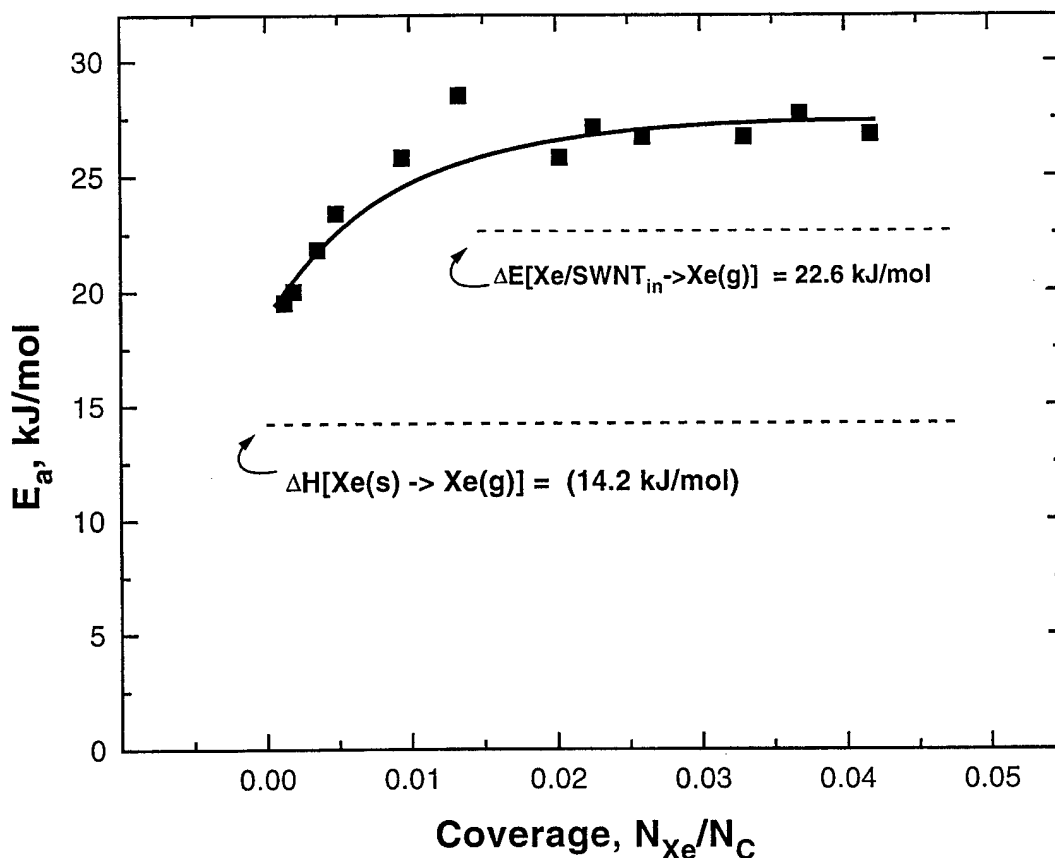
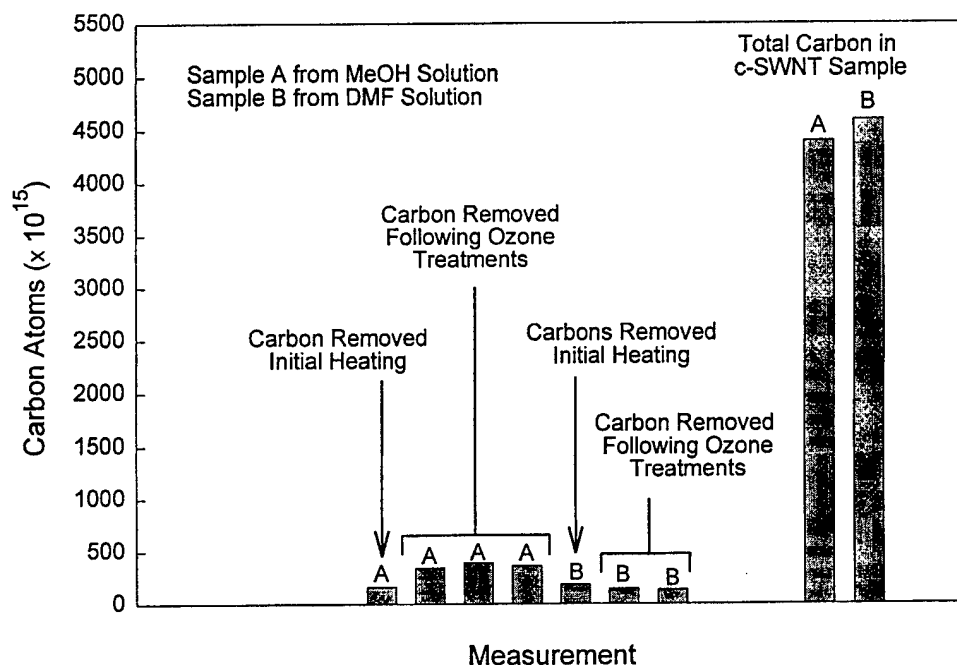


Figure 25. Activation energy for Xe desorption from o-SWNT [7]. The 22.6 kJ/mol calculation was done for zero coverage Xe.

The simulations show that Xe cannot adsorb appreciably on the outer surface of the o-SWNT under the Xe flux conditions employed here. Furthermore, adsorption in the interstitial regions between SWNTs is not possible for the Xe atom because of its large size. In addition, the saturation coverage we have measured at 95 K (coverage = 0.042 Xe/C) is in good agreement with the simulations where a saturation internal coverage of 0.06 Xe/C was calculated for the exposure range used. This coverage corresponds closely to the density of Xe(s), indicating that the capacity of the interior of the o-SWNTs has reached its maximum possible value.

The Xe desorption kinetic curves shown in Figure 21 display a common leading edge, independent of Xe coverage. This is indicative of zero-order desorption kinetics. Such kinetics are usually associated with a phase transition in the adsorbed layer which drives the desorption process. Speculations about the origin of the zero-order kinetics have been made by us, involving an equilibrium between quasi 1-D Xe inside the nanotubes and a low equilibrium coverage of 2-D Xe on the outer surface of the SWNTs. These ideas await theoretical examination.

There is much interest in the presence of defect sites on SWNTs. We have devised a method to measure the atomic fraction of these sites by measuring the evolution of CO and CO<sub>2</sub> during annealing [10]. The CO and CO<sub>2</sub> evolution is compared to that produced by total combustion of the SWNTs in O<sub>2</sub>. Annealing to 1073 K converts the oxygenated defect sites to carbon-dangling bond sites. These measurements were made on the SWNTs as received, and also after sequential reoxidation of the carbon-dangling bond defect sites with O<sub>3</sub>. It is found that about 5% of the carbon atoms are linked to O atoms in the SWNT material from the Rice group, after oxidative acid treatment. A summary of the data is given in Figure 26.



**Figure 26.** The amount of carbon evolved as gaseous CO<sub>2</sub> and CO following various treatments [10]

The presence of 5% defect sites on the original SWNT samples suggests that the use of this type of material as a basis for nanoelectronic technologies will face difficulties, since the assumptions made about the electronic structure of the ideal SWNTs will certainly differ from SWNT material containing this large fraction of defects. The oxygenated defects must be located both at the ends of the nanotubes where free carbon valencies are available, as well as on the walls. A 5% oxygenated defect level could not be achieved by oxidation of the ends alone.

In the course of this work, we have employed almost pure O<sub>3</sub> to oxidize SWNTs. This is a superb method to titrate the carbon-dangling bond defect sites, and transmission IR spectroscopy detects the formation of ester and quinone groups by this treatment.

Since the SWNTs have been activated at 1073 K and surface-bound H has been eliminated (mainly as  $\text{CH}_4$ ), it is of interest to see that  $-\text{COOH}$  groups are not produced by the  $\text{O}_3$ . The development of the oxygenated surface species is shown in Figure 27, where the infrared spectra show these spectral changes during ozonolysis. We believe that the titration of surface defect sites on SWNTs by  $\text{O}_3$  will provide a chemical handle for functionalization of SWNT material at these sites.

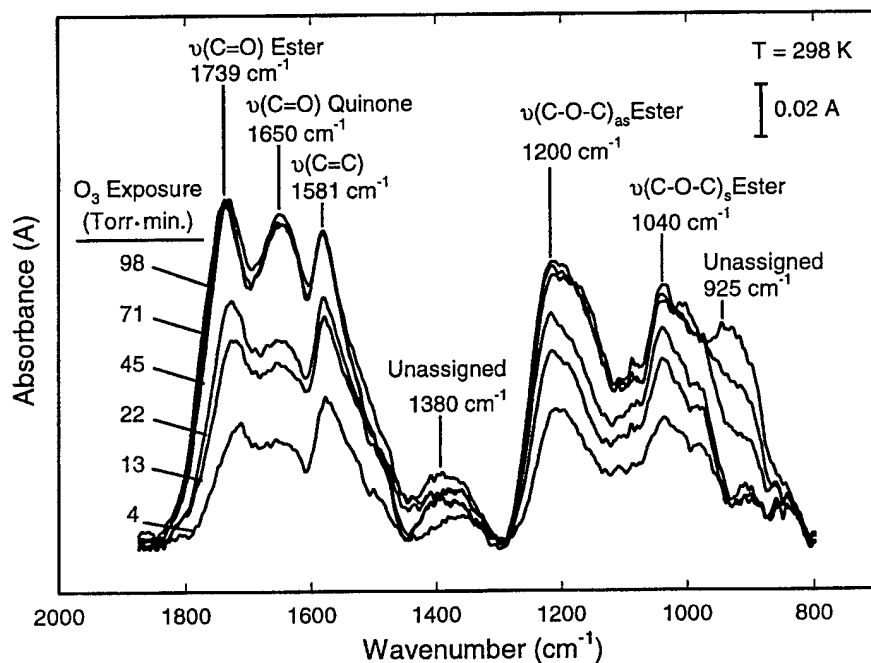


*Figure 27. Formation of oxygenated groups on SWNTs during ozonolysis [11]*

The majority of the oxidized surface functionalities may be removed by annealing to 1073 K, and a sequence of spectra and difference spectra are shown in Figure 28 for the temperature range 473 – 1073K.

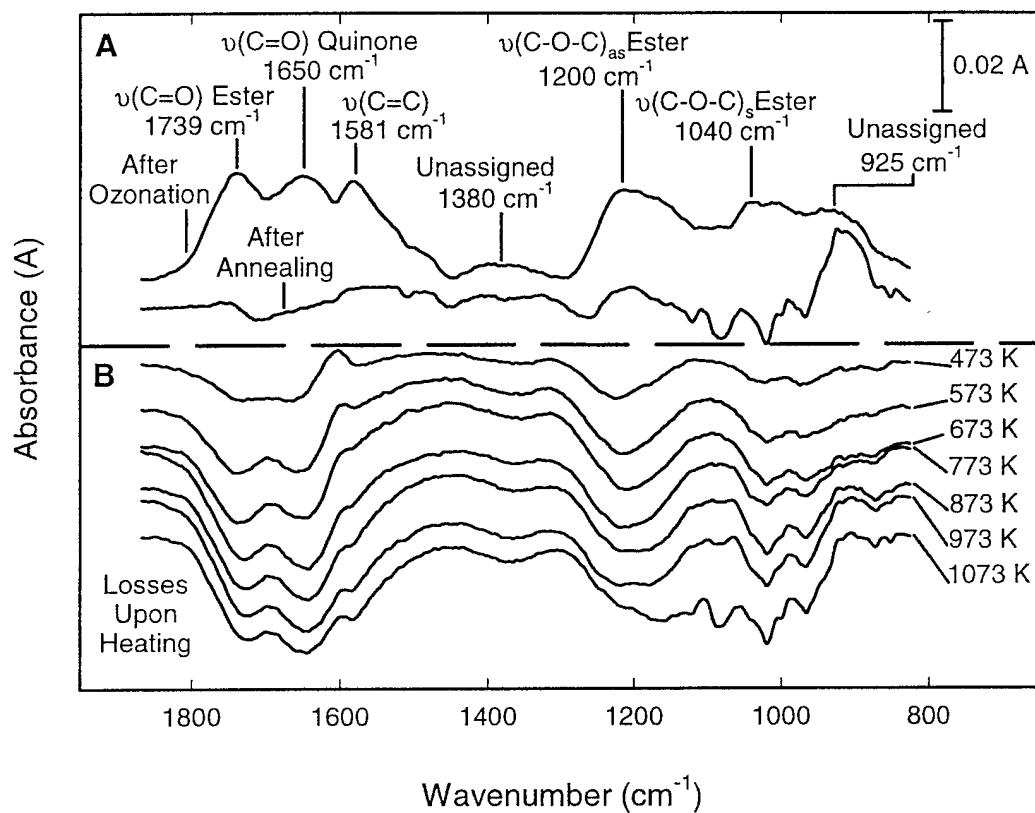


**Figure 28.** *Thermal decomposition of oxygenated carbon species produced by  $O_3$  on SWNTs [11].*

The capabilities for the study of oxidized surface functionalities on SWNT material has been extended in exploratory studies to amorphous carbon and soot samples [12]. The interaction of soot with  $O_3$  is quite interesting, and our studies have clarified some questions which have existed in the atmospheric/environmental community. Figure 29 shows an infrared spectral comparison between the ozonized SWNT material and ozonized amorphous C. It is of interest to note that the sharp spectral bands seen for the more well-defined SWNT material may be associated with analogous carbonyl bands on the soot which are much broader. This is probably due to the more homogeneous character of the SWNT molecules compared to the ill-defined amorphous carbon material.

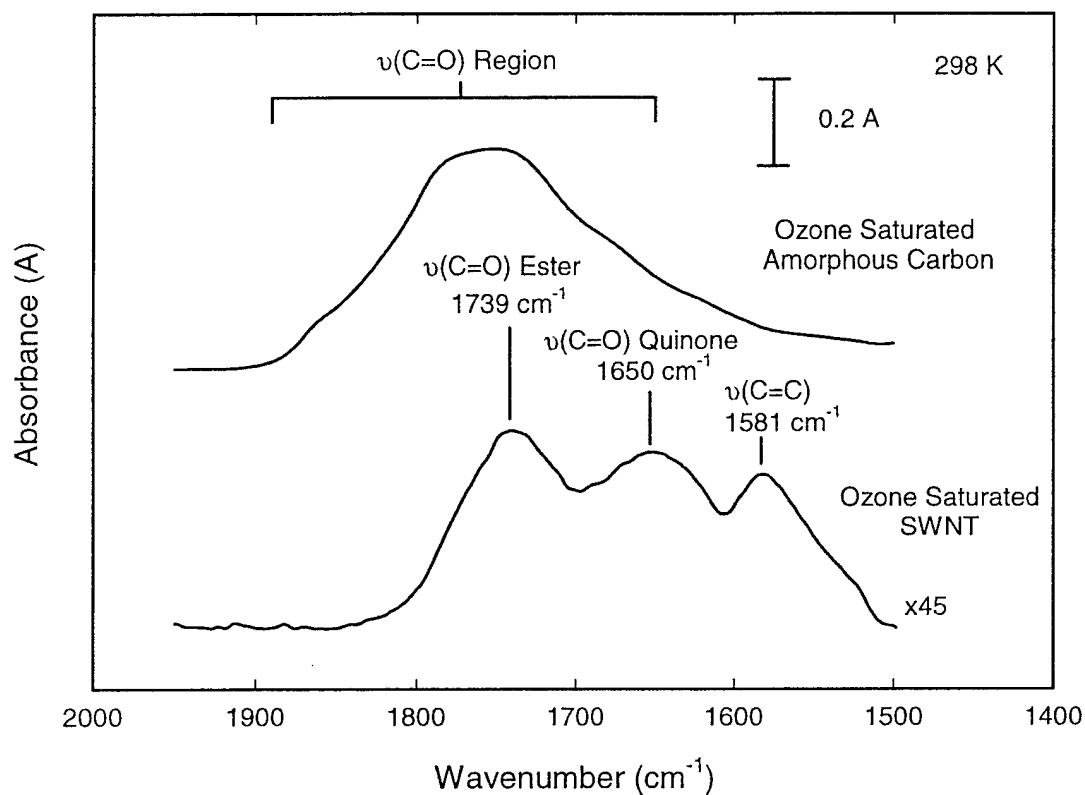


**Figure 29.** Comparison of the IR spectral for ozonized SWNT material and amorphous carbon material [12].

#### G. Summary of Publication Activity: 1997- 2001

The following papers have been published or submitted under ARO support during the 34 months of this contract:

517. D. C. Sorescu and J. T. Yates, Jr., "The Adsorption of CO on the TiO<sub>2</sub>(110) Surface: A Theoretical Study," *J. Phys. Chem.* **102**, 4556 (1998).
527. D. V. Heyd, R. J. Scharff and J. T. Yates, Jr., "Comparison of Thermal and Photochemical Behavior of O<sub>2</sub> Chemisorbed on Pt(335)," *J. Chem. Phys.* **110**, 6939 (1999). Erratum: *J. Chem. Phys.* **111**, 1340 (1999).

541. J. Zhuang, C. N. Rusu and J. T. Yates, Jr., "The Adsorption and Photooxidation of CH<sub>3</sub>CN on TiO<sub>2</sub>," *J. Phys. Chem. B* 103, 6957 (1999).
542. I. Lyubinetsky, S. Mezhenny, W. J. Choyke and J. T. Yates, Jr., "STM Assisted Nanostructure Formation: Two Excitation Mechanisms for Precursor Molecules," *J. Appl. Phys.* 86, 4949 (1999).
551. D. B. Mawhinney, V. Naumenko, A. Kuznetsova, J. T. Yates, Jr., J. Liu and R. E. Smalley, "Infrared Spectral Evidence for the Etching of Carbon Nanotubes: Ozone Oxidation at 298 K," *J. Amer. Chem. Soc.* 122, 2383 (2000).
552. C. N. Rusu and J. T. Yates, Jr., "Photochemistry of NO Chemisorbed on TiO<sub>2</sub>(100) and TiO<sub>2</sub> Powders," *J. Phys. Chem. B* 104, 1729 (2000).
554. A. Kuznetsova, D. B. Mawhinney, V. Naumenko, J. T. Yates, Jr., J. Liu and R. E. Smalley, "Enhancement of Adsorption Inside of Single Walled Nanotubes – Opening the Entry Ports," *Chem. Phys. Lett.* 321, 292 (2000).
555. D. C. Sorescu, C. N. Rusu and J. T. Yates, Jr., "The Adsorption of NO on the TiO<sub>2</sub>(110) Surface: An Experimental and Theoretical Study," *J. Phys. Chem. B* 104, 4408 (2000).
556. A. Kuznetsova, J. T. Yates, Jr., J. Liu and R. E. Smalley, "Physical Adsorption of Xenon in Open Single Walled Carbon Nanotubes – Observation of a Quasi 1-D Confined Xe Phase," *J. Chem. Phys.* 112, 9590 (2000).
559. D. B. Mawhinney, V. Naumenko, A. Kuznetsova, J. T. Yates, Jr., J. Liu and R. E. Smalley, "Surface Defect Site Density on Single Walled Carbon Nanotubes by Titration," *Chem. Phys. Lett.* 324, 213 (2000).
568. D. B. Mawhinney and J. T. Yates, Jr., "FTIR Study of the Oxidation of Amorphous Carbon by Ozone at 300 K – Direct COOH Formation," *Carbon*, in press.
569. A. V. Walker and J. T. Yates, Jr., "Does Cuprous Oxide Photosplit Water?" *J. Phys. Chem.* 104, 9038 (2000).
572. C. N. Rusu and J. T. Yates, Jr., "Adsorption and Decomposition of Dimethyl Methylphosphonate on TiO<sub>2</sub>," *J. Phys. Chem. B* 104, 12292 (2000).
574. C. N. Rusu and J. T. Yates, Jr., "Photooxidation of Dimethyl Methylphosphonate on TiO<sub>2</sub> Powder," *J. Phys. Chem. B* 104, 12299 (2000).
575. V. V. Simonyan, J. K. Johnson, A. Kuznetsova and J. T. Yates, Jr., "Molecular Simulation of Xenon Adsorption on Single-Walled Carbon Nanotubes," *J. Chem. Phys.* 114, 4180 (2001).

## **H. Summary of External Interactions Involving U.S. Army Research Interests**

### **1. Aberdeen Proving Ground**

Studies of the infrared spectroscopy of adsorbates inside carbon single walled nanotubes have been initiated with support from Dr. David Tevault of Aberdeen Proving Ground.

### **2. Guild Associates**

Four papers were written as a result of research support from Guild Associates, in collaboration with Dr. Joseph Rossin. The papers were collaboratively produced, and Dr. Karl Gerhart of Aberdeen Proving Ground was a coauthor on each. This work concerned the activation of  $\text{Al}_2\text{O}_3$  for the destruction of chemical agents. Application for a joint patent was made.

## **I. Scientific Personnel Supported**

1. Dr. Amy V. Walker
2. Ms. Camelia Rusu (Ph.D. 2000)
3. Mr. Junning Zhuang
4. Ms. Anya Kuznetsova (Ph.D. 2001)

## **J. Scientific Progress and Accomplishments**

(See main text)